Holocene climate variability:

A proxy based statistical overview

Master's Thesis

Faculty of Science

University of Bern

Presented by

Christian Grob

2009

Supervisor:

Prof. Dr. Heinz Wanner

Institute of Geography, University of Bern

And

Oeschger Centre for Climate Change Research

Co-Supervisor:

Dr. Simon Scherrer

Federal Office of Meteorology and Climatology MeteoSwiss, Zurich

Wissenschaft ist die Voraussicht von Wiederholungen.

Antoine de Saint-Exupéry

Abstract

Although the climate since the last glacial period is relatively stable in comparison with the larger variations from glacial to interglacial periods, there are considerable fluctuations on different spatial and temporal scales. Bond et al. [2001] suggested the existence of a millennial-scale cycle in the North Atlantic climate throughout the Holocene. Numerous climate proxies in various regional climatic sub-systems have since then been related to this possible cycle.

This study aims to compare a set of 40 climate proxies from all continents with the help of change point analysis and a method to detect rapid climate change for the past 12000 years. Furthermore, the two eye-catching clusters of changes are set in a spatial context and possible forcing mechanisms and patterns of change are illustrated. In addition, the changes in the North Atlantic region are focused and linked to previous studies.

The results indicate that the two focused large-scale changes centered at 2.8 and 6.4 kyr BP are likely to be related to low solar activity and that these centennial-scale changes follow the El Niño – Southern Oscillation and North Atlantic Oscillation patterns, however some of the characteristics occur to be dominated by the low solar activity itself.

The analyses in the North Atlantic region showed quasi-periodic patterns in the first half of the Holocene, likely caused by meltwater outbreaks, which reduced the thermohaline circulation in the North Atlantic. The indications of a cycle however become indistinct in the past 6000 years, which is why the existence of a pervasive cycle appears questionable.

Acknowledgements

Above all, I would like to thank Prof. Dr. Heinz Wanner. He not only supported my work on a scientific level but also encouraged me, when I felt overstrained. His infecting enthusiasm and the helpful advices he gave, kept me motivated to finish this challenging thesis. Despite his numerous obligations, he always found time to provide advice when problems arose.

Furthermore, I want to thank my Co-Supervisor, Simon Scherrer, who helped me through the initial difficulties of programming a script for the change point analysis.

Sincere thanks go to all the members of the climatology and meteorology research group at the University of Bern. They assisted me to cope with the everyday problems of a “junior climate scientist” and we had a great time together.

Further thanks go to Nina for her never-ending emotional support and distraction during the stressful last year.

Last but not least, I want to thank my parents, who have supported me throughout my entire academic studies.

Without the help of all the mentioned people, this thesis could not have been completed! Thank you very much!

List of Figures

List of Tables

Abbreviations

AD	Anno Domini
Asl	Above sea level
BP	Before present (with reference to 1950 AD)
CUSUM	Cumulative Sum Charts
EAM	East Asian Monsoon
ENSO	El Niño – Southern Oscillation
EPICA	European Project for Ice Coring in Antarctica
GISP2	Greenland Ice Sheet Project 2
GRIP	Greenland Ice Core Project
HSG	Hematite Stained Grains
IOD	Indian Ocean Dipole
IPWP	Indo-Pacific Warm Pool
IRD	Ice-rafted Debris
ISM	Indian Summer Monsoon
ITCZ	Innertropical Convergence Zone
K	Kelvin
kyr	Kiloyear = 1000 calendar years
LIA	Little Ice Age
NAO	North Atlantic Oscillation
NGRIP	North Greenland Ice Core Project
PNA	Pacific – North America Pattern
RCC	Rapid Climate Change
SD	Standard Deviation
SMOW	Standard Mean Ocean Water
SST	Sea Surface Temperature
TSI	Total solar irradiance at the top of the atmosphere
YD	Younger Dryas

Table of Contents

1 Introduction

1.1 Holocene climate: an overview

Since the beginning of the industrialization in the second half of the 18th century human influence on ecosystems drastically increased. There is very high confidence that human activity has had a net effect of warming since 1750 AD [*IPCC*, 2007], although it is still debated how much of the recent global warming can be allocated to human influence and how much to natural variability.

The climate in the Holocene is defined as the time span between the termination of the Younger Dryas (YD), which was the final stadial of the last glaciation and ended about 11.7 kyr BP ago. It was often described as a climatically stable period [*Dansgaard et al.*, 1993]. This conclusion was drawn of relative isotope concentrations in Greenland ice sheets, which appeared to be fairly stable on centennial to millennial time scales during the Holocene. This relative stability stood in sharp contrast to the rigorous Dansgaard / Oeschger cycles observed during the last glacial period.

Nevertheless, recent and well-dated studies now show distinct climate variations during the Holocene, although their amplitudes and dominant periods are still under discussion [*Bond et al.*, 1997]. Although these findings motivated researchers to explore further temporally highly resolved climate proxies in order to subdivide the Holocene in different periods with matchable conditions, the periods are not consistently grouped. Very broadly however, the climatic Holocene epochs coincide largely with three chronozones [*Nesje and Dahl*, 1993; *Wanner et al.*, 2008]. The first epoch after the YD coincides with the Preboreal and Boreal and lasted from about 11.6 to 9 kyr BP. It was followed by the Atlanticum, which was manifested as a warm and moist period in the mid- to high latitudes. It covered the time from about 9000 to 6000-5000 years BP and is often referred as Holocene climate optimum and Alti- or Hypsithermal. The following rather cold phase was characterized by several glacier advances is often called Neoglacial corresponds with the Subboreal and Subatlantic stratigraphic sequence and lasted until the beginning of industrialization [*Wanner et al.*, 2008].

Since that time, global temperatures are increasing and since 1990 they have been higher than at any time during the last 1000 years [*Crowley*, 2000; *Esper et al.*, 2002; *Jones and Mann*, 2004; *Mann et al.*, 1999; *Moberg et al.*, 2005; *Osborn and Briffa*, 2006; *Wanner et al.*, 2008]. Additionally several research teams have shown that it is no longer possible to explain the abrupt temperature rise since the beginning of industrialization only with natural forcing

factors. The man-made increase of greenhouse gas concentrations plays a crucial role for the interpretation of this recent warming [*Ammann et al.*, 2007; *Bütikofer*, 2007; *Crowley*, 2000; *Hegerl et al.*, 2003; *Jones and Mann*, 2004; *Stott et al.*, 2000; *Tett et al.*, 1999].

1.2 Climate Variations

1.2.1 The nature of climate variations

The climate system varies in different ways. The most obvious one is a linear or exponential transition, just like it seems to have occurred in the last decades, moving from a stable state to an other stable state under the influence of forcing factors which affect the system over a certain period. This results in a change in the mean of a specific climate parameter. Assuming linearity, the results of these forcings can be well calculated and predicted. Since the climate system underlies several non-linear feedbacks drastic changes can occur if a critical threshold is exceeded.

Climate variability can also be the response to rapid impacts on the climate system, e.g. after volcanic eruptions. Depending on the stability of a system, it recovers after a certain time period (resilience) or finds another equilibrium state. Although such events seem to be random in time and space, a number of studies have shown that in some circumstances the impacts on climate can be predicted, even though the eruptions themselves are non-periodic [*Hansen et al.*, 1996]. Furthermore, climatic variability can be characterized by an increase in variance in addition to or apart from a change in mean.

Finally, climatic variation may be characterized by periodic and hence predictable cycles. Since the forcing factors are manifold and varying in time, the variability of the climate system cannot be specified by one of the aforementioned types. Additionally, the types of variability change with a shift in perspective: apparent trends of decades are potential cutouts of long-time cycles or random phenomena of internal variability of the climate system. Climatic variability is an extremely important climate characteristic with respect to society, since an increase in variance is equal to an increase in unexpected weather occurrences [*Bradley*, 1996].

1.2.2 Physical proxy records

Since instrumental measurements only reach back about 130 to 240 cal yrs, it is crucial to find other ways to get information about past climate [*Pfister et al.*, 1999]. So-called proxy data is used in paleoclimatology to study the climate prior to the period of instrumental measurements. Proxy records are generated by climate-dependent natural phenomena and therefore provide information about past climate. They are largely grouped in documentary

(man-made) and natural archives. This thesis deals with natural proxies only, since civilization and therefore man-made proxies only exist at the very end of the Holocene. Archives in nature incorporate climate-related phenomena into their biological, chemical or physical structure. To extract the paleoclimatic signal from proxy data, the record must first be calibrated. Calibration involves using modern climatic records and proxy materials to understand how, and to what extent, proxy materials are climate dependent [*Pfister et al.*, 1999]. All climatic reconstructions are therefore based on studies of climatic dependency in natural phenomena today. The interpretation is often hampered by the fact that the characterization of the proxy is commonly defined by more than one single influencing environmental parameter. Additionally, homogeneity is not always given since the environmental situation may have changed over time. The 'transfer-function' from proxy- to climate-value is hence not stable in time. For reliable paleoclimatic reconstructions it is therefore crucial that contemporary processes in the climate system are well understood [*Bradley*, 1996].

A special case of changing the environment of the proxy is the human interference with the environment in the past decades to centuries, which complicates the assessment of natural climate change on the basis of proxies and its separation from human-induced changes [*Versteegh*, 2005].

Though working with proxies holds these pitfalls, they are crucial in the exploration of past climate since they are the only way to get information about it.

1.2.3 Climate forcing

In order to find out more about the main forcing factors and their individual influence on the climate system, it is necessary to differentiate between different types of forcing. Very often, studies assume a change in one forcing only, ignoring the intrinsic climatic variability under constant and multiple forcing [*Versteegh*, 2005].

The following types of forcings occur:

- Exogenic processes modulate forcing from outside the influencing its climate (e.g. solar variability, supernovae, changes in Earth's orbital parameters).
- Endogenic processes modulate forcing from inside the Earth system (e.g. volcanism, continental drift and geomagnetism).
- Autogenic processes encompass climate variability even if exogenic and endogenic forcings are held constant. They include the feedback mechanisms within the spheres of the climate system (e.g. within or between atmosphere, hydrosphere, biosphere, cryosphere and land surface) [*Versteegh*, 2005].

1.2.3.1 Milankovich forcing throughout the Holocene

The sun plays a central role for the Earth in at least two respects: Firstly it is the gravitational center around which the globe orbits elliptically, and, secondly, the sun is by far the most important source of energy for the Earth system [*Beer et al.*, 2006]. The amount of solar radiation arriving at the top of the atmosphere depends on two factors: on the amount of energy emitted at the sun and on the distance and orientation of the Earth to the sun. The latter is first described and explicitly calculated by Milutin Milankovich [1930].

The changes in Earth's distance and orientation to the sun result from the influence of other planets in the solar system, mainly Jupiter and Saturn, on Earth's orbit around the sun, from changes in the mean tilt angle of the Earth's axis relative to the ecliptic plane, and from the precession of the Earth's rotational axis around the mean axis.

The prece

The change in excentricity of the Earth orbit has dominant periodicities of about 100 kyr and 400 kyr and is strongly influencing the differences between summer and winter temperature. Additionally, the yearly mean insolation declines with an increase of excentricity, even though this decrease is minor [*Roedel*, 1994]. The tilt angle of the Earth axis with respect to the ecliptic (plain of the Earth orbit around the sun) varies with a 40 kyr cycle between 22.1° and 24.5°. The larger the tilt, the stronger is the contrast between summer and winter insolation. Since the Earth is no ideal sphere but rather a rotational ellipsoid, the sun and the moon exert a torque on the tilted Earth axis, inducing a lateral precession of the Earth axis. This precession causes a shift in seasonal occurrence of perihelion and aphelion with a main periodicity of 23 kyr [*Roedel*, 1994].

Orbital forcing is the only forcing that can be calculated precisely for the past and even for the time frames of future several million years because it is based purely on celestial mechanics [*Beer et al.*, 2006; *Laskar et al.*, 2004].

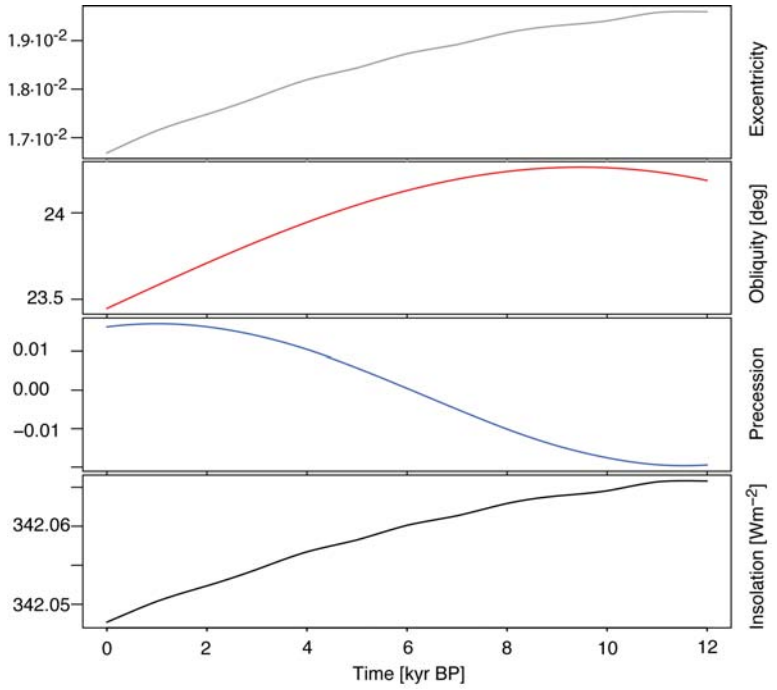

Figure 1: Global Milankovich parameter change throughout the Holocene [*Laskar et al.*, 2004].

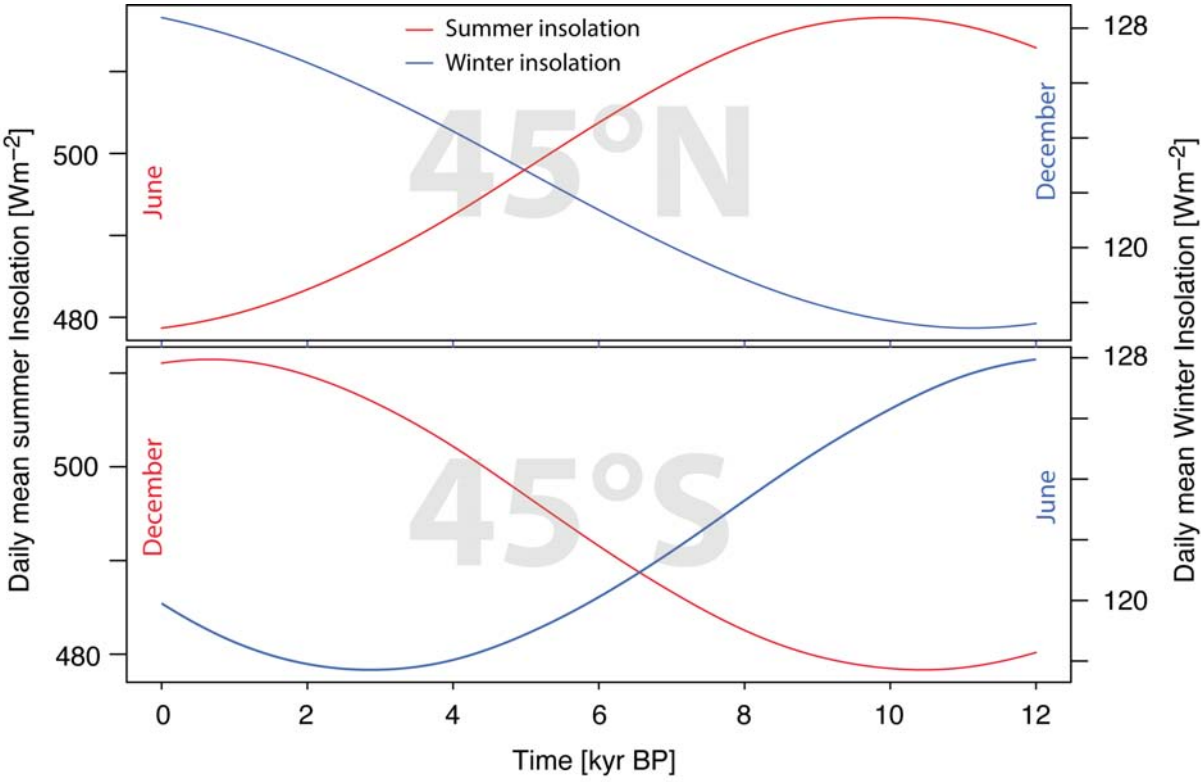

Figure 2: Daily mean summer (red) and winter (blue) insolation throughout the Holocene [*Laskar et al.*, 2004].

Figure 1 depicts the changes in Earth parameters throughout the past 12 kyr. Figure 2 focuses on the solar insolation changes due to Earth orbit changes. Most consequence on the global insolation changes has the change in excentricity, which describes the ratio of the semi-major to the semi-minor axis of the Earth's elliptic orbit around the sun. It decreases steadily during the entire Holocene, resulting in a marginal decrease of total insolation.

After a slight increase in the axial tilt at the beginning of the Holocene, it started to decrease more than 0.5° leading to a weaker contrast between summer and winter insolation on both hemispheres.

The precession induced a shift in the date of the perihelion from summer towards winter Currently, the perihelion is on January 3, therefore the differences in summer and winter insolation on the northern hemisphere is slightly damped compared to a phase with the perihelion during the summer months. On the southern hemisphere it is vice versa [*Bauer*, 2005].

Figure 2 shows the seasonal hemispheric insolation changes at 45° North and South mainly induced by the precession of the Earth axis. On the Northern Hemisphere the summer insolation slightly increased by the beginning of the Holocene with a peak around 10 kyr BP and decreased by 37 Wm^{-2} to the present. The northern hemispheric winter insolation shows a change in the opposite direction with a steady increase since the beginning of the Holocene. The southern Hemisphere shows a parabolic increase of summer insolation since 10 kyr BP and decreasing winter isolation until 2.5 kyr BP, and a damped increase in both summer and winter isolation in the last 2500 calendar years [*Laskar et al.*, 2004].

1.2.3.2 Solar variability

Figures 1 and 2 assume a steady total solar irradiance (TSI) of 1368 Wm^{-2}. Since the solar emission of radiation is varying, the insolation at the top of the atmosphere is therefore not to be assumed as a constant. Reconstructing past changes of the solar constant is much more challenging than calculating the aforementioned forcing induced by changes in Earth axis parameters [*Wanner et al.*, 2008].

Satellite based radiometer measurements show a correlation between the 11-year sunspot cycle and the solar irradiance. The changes however are too small to affect Earth's climate severely [*Beer et al.*, 2000]. The measured changes within the last two cycles were 0.1% only, what corresponds to a radiative forcing of 0.24 Wm^{-2} [*Wanner and Bütikofer*, 2008]. There are indications that on larger timescales the variations are much bigger, although there is no final answer on this problem yet. Reconstructing the long-term solar variability is performed with the use of cosmogenic radionuclides like ^{14}C and ^{10}Be stored in ice cores. They are

produced by cosmic rays in the atmosphere. The intensity of the cosmic radiation and therefore the production rate of cosmogenic nuclides depends on the solar activity. The archives provide information on the solar magnetic activity and offer the opportunity to extend the short-term reconstructions based on sunspot and faculae observations up to 10 kyr [*Beer et al.*, 2006; *Steinhilber et al.*, 2009].

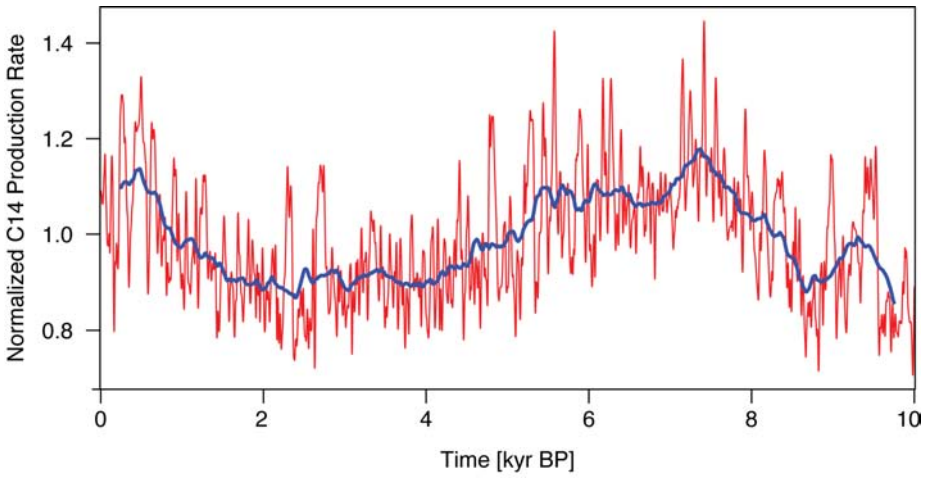

Figure 3: Reconstruction of the normalized ^{14}C production rate.

Figure 3 depicts a reconstruction of the ^{14}C production rate, which is an indirect measure for the solar activity. It was calculated using the Bern3D dynamic ocean carbon cycle model [*Muscheler et al.*, 2007]. Since the relationship of ^{14}C and solar activity is still unknown and probably non-linear, relative units are used. The blue curve depicts a 500 cal yrs running-mean filter.

1.2.4 Volcanic activity

During large volcanic eruptions, considerable quantities of sulfuric gases are injected various levels of the atmosphere. Those gases have the capability to cool, or in special cases, warm the atmosphere by 0.2 – 0.3 K for several years after the eruption [*Robock*, 2002; *Zielinski*, 2000]. Compared to the sulfuric gases the impact of $C0_2$ and water vapor to the climate is negligible. Because the silicate matter of eruptions is much larger and heavier, the ash compound settles more quickly and its effect on climate is also unimportant.

The sulfuric gases and their derivates affect the climate system in multiple ways. On one hand, they can lead to ozone depletion, on the other hand sulfuric gases lead to climatic perturbation in the form of cooling at the Earth's surface as incoming solar radiation is either reflected or absorbed in the stratosphere. This results in stratospheric warming and hence in

tropospheric warming [*Zielinski*, 2000]. The radiative forcing sums up to 5 Wm^{-2} [*Crowley*, 2000].

An overview of volcanic activity and its total impact on climate throughout the entire Holocene is still a matter of further research.

1.3 A pervasive millenial-scale cycle in North-Atlantic Holocene climate

In 1995 O'Brien derived from measurements of soluble impurities in Greenland ice that the Holocene atmospheric circulation above the ice cap was punctuated by a series of millennial-scale shifts. The most prominent of those shifts appeared to correlate with Denton and Karlen's [1973] glacial advances. Encouraged by this finding, Bond et al. [1997] launched an investigation of Holocene deep sea sediments in the North Atlantic. They expected that the shifts in atmospheric circulation above the ice cap were part of much larger climate pattern, which left its imprint in the deep-sea record.

They analyzed cores from the ocean sediment off the west coast of Ireland and further in the Northwest between Iceland and Greenland. High-resolution radiocarbon datings showed that both cores have nearly complete Holocene sections and were sampled at intervals of 0.5 to 1 cm, which is equivalent to 50 to 100 cal years. They ascertained the concentrations and the percentages of certain types of lithic grains. Figure 4 shows a stack of four sediment cores and depicts a series of rises in grain concentrations and concurrent increases in volcanic tracers stemming from Iceland or Jan Mayen and hematite-stained grains (HSG) originating from the east coast of Greenland were found. Bond and his team hence concluded that ice-rafting episodes also occurred during the Holocene and that the North Atlantic climate since the last glacial must have undergone a series of abrupt reorganizations, each with sufficient impact to force concurrent increases in debris-bearing drift ice at sites more than 1000 km apart and overlain today by warm, largely ice-free surface waters of the North Atlantic. The events with enhanced ice-rafted debris (IRD) reveal peaks at 0.5, 1.4, 2.8, 4.2, 5.9, 8.1, 9.4, 10.3, and 11.1 kyr BP. Bond suggested that the direct reason for the enhanced ice rafting was a series of ocean surface cooling events induced by a considerable change in the thermohaline circulation in the North Atlantic [*Bond et al.*, 1997]. Since these events occurred about every 1500 ±500 years and persisted over millennia, a 1500-years cycle was proposed as the dominating fluctuation of Holocene's climate, analogously to the Dansgaard / Oeschger events during the last glacial period and based on the same forcing mechanisms but with a change in amplitude.

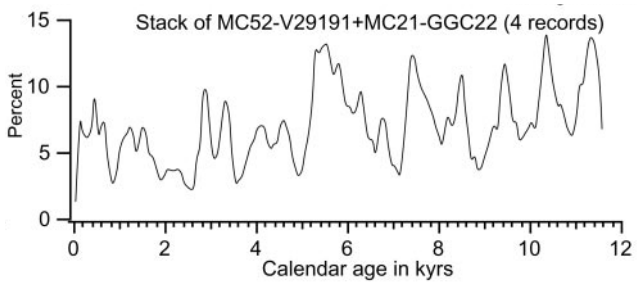

Figure 4: Holocene records of drift ice; Stack of four sediment cores expressed as percentages of lithic grains [*Bond et al.*, 2001].

Since the most recent of the cooling periods, the Little Ice Age (LIA) [e.g. *Matthes*, 1939] ended in the late 19th century, some of the current global warming could be associated with the millennial-scale Bond-cycle [*Bütikofer*, 2007]. The knowledge about the processes and the behavior of natural climate variability in the Holocene is however not enough founded to subdivide the anthropogenic and natural fraction of the recent global change, nor is the science ready to predict future influence of the millennial-scale cycle to Earth's climate. Since naturally occurring and man-made climate fluctuations have had a considerable impact on civilization as described using the example of prolonged drought periods [*deMenocal*, 2001], and will have in the future [*IPCC*, 2007], it is crucial to expand the knowledge about past climate variability on millennial timescale.

After establishing the theory about the Bond cycles, numerous studies from many sites have been directly linked to the North Atlantic drift-ice records and the paper became one of the most cited on Holocene climate change [*Andrews*, 2006]. Mayewski et al. [2004] presented a composition of various proxies from all around the world and reckoned to see a quasi-periodic pattern of global extent coinciding with the Bond cycles, however they did not statistically confirm these findings. The lively debate about the spatial and temporal extent of the cycles is still in progress [*Andrews*, 2006; *Wanner and Bütikofer*, 2008]. Open questions still remain concerning the controversy about the forcing factors of centennial- to millennial-scale climate variability, since Milankovich-forcing (section 1.2.3.1) is widely accepted to be a key factor on 20'000- to 100'000-year timescales [*Hays et al.*, 1976] during the Pleistocene. Investigating the nature of the forcing factors, namely solar activity or large volcanic eruptions and their influence on climate is thus the current challenge in understanding Holocene climate variability.

1.4 Objectives

The lively debate about the existence, the spatial extent and the magnitude of climatic cycles is still ongoing [*Andrews*, 2006; *Bütikofer*, 2007; *Wanner and Bütikofer*, 2008]. In this thesis, we assess and compare globally distributed proxies of manifold climate factors. Unlike Bütikofer [2007] we include the entire Holocene and set the limit of our analyses to 12 kyr BP in order to be able to catch all the ice rafting events proposed by Bond [2001]. The aim is to trap and compare potential events of rapid climate change on regional and global extent and to subdivide the main phases of the Holocene using change point analysis. Evaluating spatial patterns will hopefully show one way to indications about past atmospheric circulation schemes and possible origins of the Holocene climatic cycles.

2 Data

2.1 Proxy data

As introduced above, the Bond cycles in the Northern Atlantic occur on a millennial scale. Since the aim of this thesis is to find out more about the cyclicities in Holocene climate, it is crucial to work with data going back to at least 12 kyr BP. The prevalent paleoclimatic records and reconstructions with high temporal resolution (<200 cal years) were favored. We tried to find data representing not only the North Atlantic region but all the regions of the world. Most of the data used in this thesis is available on the IGBP PAGES/WDG for paleoclimatology, which provides data about past climate and environment derived from a diverse range of proxies.

The main criterion for the choice for the used proxy data was the coverage of the past 12 kyr in high temporal resolution. Since detecting phases of rapid climate change is the aim of this thesis, the temporal resolution was decided to be below 200 cal years. High accuracy dating was furthermore important in the choice of our proxies.

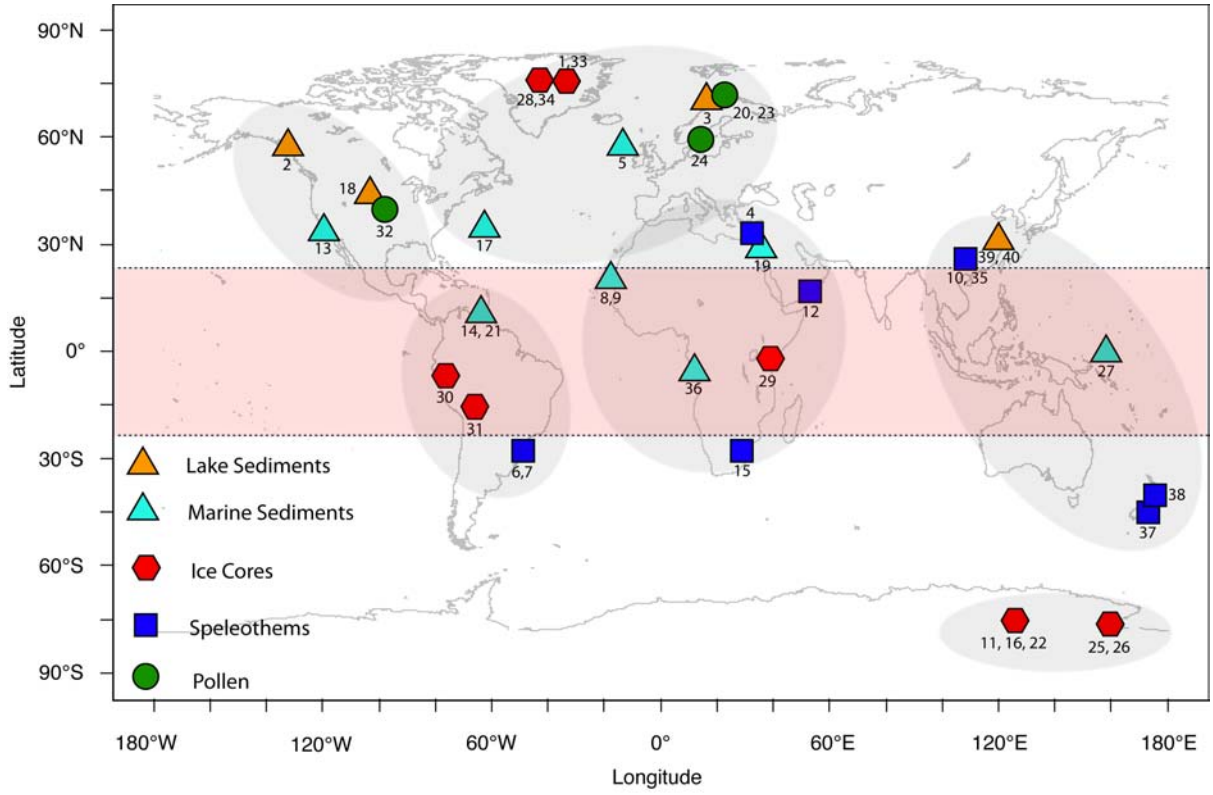

Figure 5: Map of the world showing the locations, the type and regional classification of the selected proxies (see table 1 for additional information)

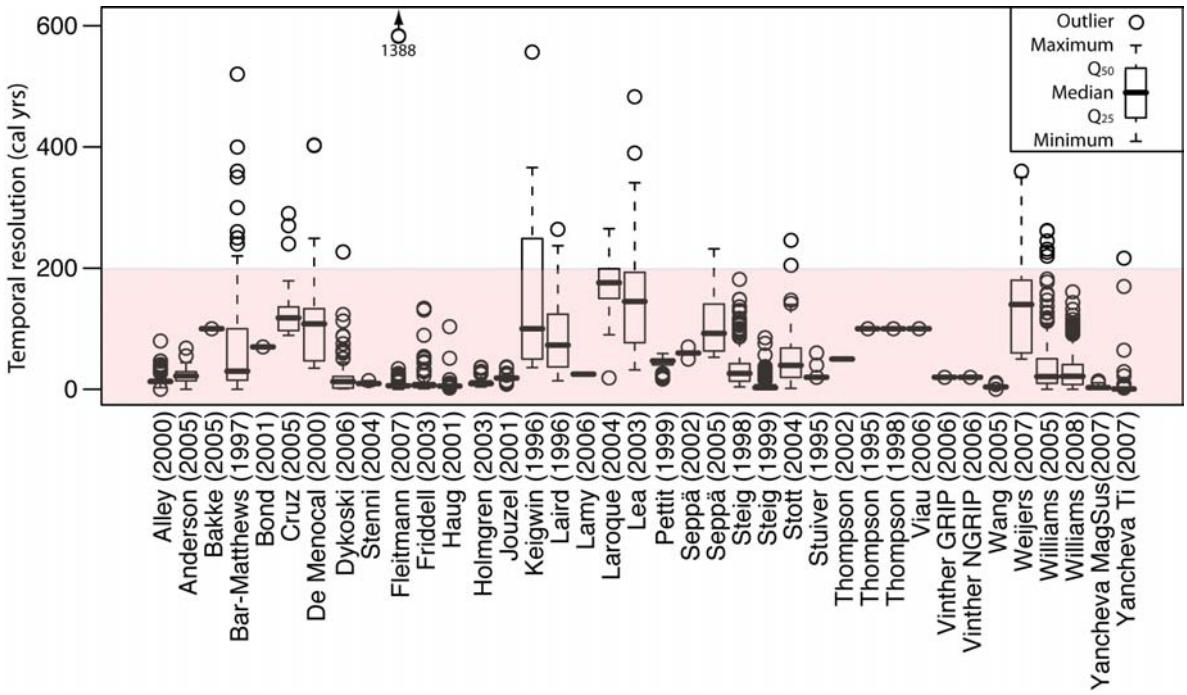

Figure 6: Box-Whisker-plot: Temporal resolution of the selected proxies.

2.1.1 Stable isotopes

In ecological systems, water is a major influencing factor. Additionally, it is a main compound in all forms of life. It is therefore crucial to study fossil water either directly in ice or indirectly through materials deposited from solution in fossil water (e.g. speleothems) to get information for paleo-environmental reconstructions. The water constituents exist in the form of different isotopes. Hydrogen has two stable isotopes with the atomic mass number of 1 and 2, so-called Protium and Deuterium. Oxygen isotopes have the mass numbers of 16, 17 and 18. Consequently, water molecules may exist as any one of nine possible isotopic combinations. However, as water with more than one heavy isotope is very rare, generally only four major isotopic combinations are common and only two of them are important in paleoclimatic research ($^{1}H^{2}H^{16}O$, generally written as HDO, and $^{1}H_{2}{}^{18}O$).

The unit for measuring ^{18}O concentrations is the excess of the $^{18}O/^{16}O$ ratio relative to a defined standard in per mill. The universally accepted standard is known as Standard Mean Ocean Water (SMOW) and was defined by Craig [1961].

Since the vapor pressure of the water with heavy isotopes is lower than that of common water, the vapor from a water body is poorer in Deuterium and ^{18}O than the initial water. Reversely, the condensation will be enriched in the heavy isotopes compared to the vapor. Consequently,

archives of past Deuterium and ^{18}O concentrations can be used as a physical proxy for temperature.

2.1.2 Ice core data

The deposition of snowfall in the cryosphere of the world provides an extraordinarily valuable record of paleoclimatic and paleo-environmental conditions. The physical and chemical study of core samples of ice and firn, taken in glaciers or ice sheets, allows drawing conclusions about the past environment. On ice sheets, snow is deposed every year and the melt and sublimation is extremely low so that snow accumulation has been continuous, in certain areas for several hundred thousand years. The information deduced from core samples is manifold. The accumulation rate and hence the thickness of the annual deposition is a measure for precipitation rate, but also air temperature, atmospheric composition, the occurrence of explosive volcanic eruptions, and even past variations in solar activity can be derived from ice core proxies.

Paleoclimatic information is obtained from ice cores by analysis of mainly
four factors.

- Stable isotopes of water and atmospheric O_2.
- Other gases from air bubbles in the ice.
- Dissolved and particulate matter in firn and ice.
- The physical characteristics of firn and ice.

Since this master thesis only deals with ice core proxies based on stable isotopes, the others are not characterized closer. Bradley [1996] addressed several chapters in his book about dating, influencing factors, sources of error, paleoclimatic reconstructions from ice cores.

Based on the aforementioned fractionating-process (see chapter 2.1.1), which occurs in the evaporation and condensation process, paleotemperature reconstructions can be derived provided that the $\delta^{18}O$ to paleotemperature function is correlated in an accurate way. By mischance, strong surface-based temperature inversions essentially decouple the surface from the atmospheric circulation above the ice cap. Temperatures are often much lower at the surface than at the top of the inversion. Hence, the correlation between top of inversion temperature and the $\delta^{18}O$ values is much stronger than the surface temperatures to the $\delta^{18}O$ content in snowfall [*Piciotto et al.,* 1960]. This was confirmed in several other studies [e.g. *Jouzel et al.,* 1983]. $\delta^{18}O$ based proxies hence do not represent the actual surface temperature but the temperatures in the free troposphere, where cloud condensation occurs. Furthermore, multiple drivers interfere with the temperature signal stored in $\delta^{18}O$ proxies. One important factor is the ^{18}O concentration in atmospheric precipitation, which on the other hand is

influenced by mostly the ^{18}O content of the water vapor at the start of condensation. Generally, the $\delta^{18}O$ is much lower in inland lakes than in the ocean water. Yet other influencing factors are the amount of moisture when condensating compared to the initial moisture content, the temperature at which the evaporation and condensation took place and some further disturbances [*Alley*, 2000; *Bradley*, 1996].

2.1.2.1 Ice core-based proxies used in this thesis

The northern regions are spatially well covered by different coring projects in Greenland. Alley [2000] used cores for the isotope analysis which were exploited in two of the four projects which were cored from the ice sheet to the bedrock in Greenland. They stem from the Greenland Ice Core Project (GRIP) and the Greenland Ice Sheet Project II (GISP2). Both the GISP2 and the GRIP cores have provided an enormous amount of information about the climatic and environmental history of Greenland and the North Atlantic region [*Bradley*, 1996]. There is a high correlation between the two cores up to an age of about 103 kyr BP [*Grootes et al.*, 1993]. Holocene fluctuations are relatively small, in the order of 1-2‰ and with only a little correlation between the two sites, probably because of local differences in snow accumulation and wind drifting of snow [*Bradley*, 1996]. The dataset used in our work is the paleotemperature reconstruction by Alley [2000]. The main focus of his paleotemperature research is centered on the evolution of temperature in the Younger Dryas. In his paper, he pointed to the uncertainties in his reconstruction emerging from atmospheric inversions [*Alley*, 2000].

A further core was analyzed by Jouzel et al. [2001] at the station of the European Project for Ice Coring in Antarctica (EPICA). It contained a high-resolution 27 kyr record and questions the classical picture of a temperature seesaw between Antarctica and Greenland. It aimed to find out more about the time period of the Younger Dryas about 14 kyr ago and was drilled in the seasons 1997-98 and 1998-99 in Eastern Antarctica.

The EPICA community members [2007] presented a methane and stable isotope record for the past 150 kyr with a focus on the hemispheric climatic relations. As in our other proxies, we used the $\delta^{18}O$ with reference to the SMOW.

The $\delta^{18}O$ record of the multinational research program North Greenland Ice Core Project (NGRIP) contains a highly resolved proxy for paleotemperature going back to 122 kyr BP. The site on 3080 meters asl of ice was chosen on a spot without flow distortions to extract an undisturbed ice core.

The core drilled by Petit [1999] at the Vostok station in Antarctica in East Antarctica contains the climate history of the past four glacials and interglacials back to 420 kyr BP. It unveiled

that the Holocene is by far the longest stable warm period recorded in Antarctica during the past 420 kyr.

Steig et al. [1998] investigated synchronous changes in the Antarctica and the North Atlantic. They compared their 100 kyr record, which they recovered at the Taylor Dome in Antarctica.

Stuiver [1995] analyzed the $\delta^{18}O$ content back to 16.5 kyr BP in a GISP2 core in order to investigate the role of the sun, the ocean and volcanic eruptions to Holocene climate. The bidecadal resolution unveiled close details about the ending of the last glacial.

Thompson et al. [1995; 1998; 2002] sampled ice cores in different places in low latitudes and analyzed their $\delta^{18}O$ values for Holocene temperature reconstruction. Their two cores from the col of Huascaran in north-central Andes of Peru contain a paleoclimatic history extending into the last glacial stage [*Thompson et al.*, 1995]. The second place they cored in South America was on the summit of Sajama Mountain in Bolivia where a ^{14}C dated, tropical record back to 25 kyr BP was recovered. Both time series show similar $\delta^{18}O$ trends during Holocene. Due to the larger thickness of the ice on the Sajama summit its core provides data in a higher temporal resolution [*Thompson et al.*, 1998]. The third record is based on drillings on the Kilimanjaro mountain and provided a 11.7 kyr, $\delta^{18}O$ based record of Holocene climate and environmental history for eastern equatorial Africa including three periods of rapid climate change at about 8.3, 5.2 and 4 kyr ago. Vinther et al. [2006] measured $\delta^{18}O$ values from GRIP and NGRIP in a temporal resolution of 20 yrs back to 32 kyr with advanced dating technologies.

2.1.3 Non-marine geological evidence

2.1.3.1 Lake sediments

Sediments in lakes are accumulated from their surrounding environment, and therefore sediment cores recovered from lakebeds allow drawing conclusions about past environmental changes. Basically, lake sediments contain material either brought along from outside the lake basin (allochthonous) or being generated inside the lake itself (autochthonous). Often, the accumulation rates are high so that high-resolution reconstructions are possible. Allochthonous substance is transported into the lakes by all sorts of runoffs and hold fluvial, aeolian clastic sediments, dissolved salts, terrestrial macrofossils and pollen. Autochthonous material on the other hand consists mostly of biogenic matter. Isotope fractionation processes in the lake evolving either from evaporation or precipitation can result in isotopic proxies stored in the lakebed sediments [Bradley, 1996].

Anderson et al. [2005] carried out multiple analyses of sediment cores from Jellybean Lake, a small, evaporation-insensitive groundwater-fed lake in the Yukon Territory, providing a

record of changes in North Pacific atmospheric circulation for the last 7500 cal yrs at 5- to 30-yr resolution. An increasing $\delta^{18}O$ value correlates with the strength of the Aleutian high.

Bakke et al. [2005] reconstructed the temperature and precipitation during the late glacial and the Holocene on the basis of lake sediments and morpho-stratigraphy in the region of northern Norway. They found large fluctuations in precipitation from 500 to 5000 mm/yr water equivalent.

Laird et al. [1996] reconstructed Holocene climatic conditions based on a lake sediment sampled in the Great Plains of the United States. Their analysis showed that the salinity in the sediments corresponds well with the historical records of mean annual precipitation minus evapotranspiration.

A high-resolution proxy for the East-Asian winter monsoon is presented by Yancheva et al. [2007] who investigated a high-resolution record of the magnetic properties and the titanium content of the sediments of Lake Huguang Maar in coastal southeast China. It is used as a proxy for the strength and the latitudinal position of the monsoon winds.

2.1.3.2 Speleothems

Speleothems are mineral cave deposits primarily composed of calcium carbonate, which was precipitated from ground water that has percolated through the adjacend bedrock. Speleothem formations occur in limestone caves, usually in the form of stalagmites or stalactites or uncommonly as deposits called flowstones. Particular trace elements included in the speleothems such as uranium can be used to determine the exact age of a speleothem. Other substances as pollen provide valuable information about past environmental conditions. Since minor changes in geological, hydrological, chemical or climatic conditions can stop the percolation of ground water, speleothem growth is often discontinuous and can therefore contain breaks in the proxy record. Paleoclimatic studies have focused on the timing of speleothem growth periods, their relationship to sea-level fluctuations and their isotopic composition [*Gascoyne*, 1992]. Proxies used in this thesis are based on the latter. Since air and water movements in a cave are relatively slow, the temperature of aforementioned and the bedrock is at equilibrium, approximating the mean annual surface temperature. During the deposition of calcite and formation of the speleothem isotope fractionation occurs in a degree, which is controlled by the cave temperature. Thus, the $\delta^{18}O$ content in the speleothems provides an indirect physical proxy for the surface temperature through time.

An accurately dated $\delta^{18}O$ and $\delta^{13}C$ record determined from two different caves in Northern Israel were analyzed by Bar-Matthews and her colleagues [2003]. They revealed striking similarities between these two caves. The record for the past 7 kyr shows a trend toward

increasing aridity and agrees well with climatic and archeological data from North Africa and the Middle East.

In a study in the subtropics of southeastern Brazil Cruz et al. [2005] investigated changes in tropical and subtropical atmospheric circulation by using stalagmites. They showed that the Dansgaard/Oeschger events during the last glaciation were also detectable in the tropics, where up to then the solar insolation was thought to be main driver in climate changes. The fluctuations south of the equator appear to be smaller than in the northern hemisphere.

Dykoski et al. [2005] presented a proxy for Asian monsoon over the past 16 kyr in the form of a speleothem from Dongge Cave situated in southern China. The time series shows four positive $\delta^{18}O$ events during the Holocene. All of them correlate with certain errors with climate changes in Greenland. Furthermore the proxy shows a strong connection with hydrological changes in northern South America related by changes in the position of the inner-tropical convergence zone. Yet another speleothem from the same cave has a better temporal resolution in its $\delta^{18}O$ measurements and reconstructs the East Asian Monsoon (EAM) for the past 9 kyr [*Wang et al.*, 2005]. Although the record broadly follows summer insolation, it is punctuated by eight weak monsoon events lasting about 1 - 5 centuries. One of them correlates with the 8.2 kyr event and most other phases of low monsoon activity with the North-Atlantic ice-rafting events.

Fleitmann and his team [2007] described a further proxy for the monsoon. They measured the $\delta^{18}O$ values in a speleothem from Oman and found decadal to centennial variations in Indian summer monsoon precipitation in the early Holocene, which were in phase with Greenland ice cores, indicating that early Holocene monsoon intensity is largely controlled by glacial boundary conditions. After about 8 kyr BP monsoon precipitation decreased gradually in response to changing Northern Hemisphere summer insolation with decadal to multi decadal variations in monsoon precipitation linked to solar activity [*Fleitmann et al.*, 2003]

Four stalagmites from the North Island [*Williams et al.*, 2004] and eight from the south island [*Williams et al.*, 2005] of New Zealand provided paleoenvironmental information of this area largely influenced by the subtropics as well as Antarctica. It was concluded from the North Island speleothem, that a first Holocene climate optimum occurred from 11 to 8.5 kyr BP, followed by a mid-Holocene thermal minimum from 6 to 2 kyr BP culminating around 4 - 3 kyr BP which was interrupted by at least seven short mild intervals. The late Holocene was concluded to be significantly warmer, especially from 0.6 - 0.9 kyr BP, suggesting a correspondence with the Medieval Warm Period as found in parts of Europe [*Williams et al.*, 2004]. The results of the South Island show that the general form of the $\delta^{18}O$ records found in

New Zealand is similar to that found in ice-cores in both hemispheres, but that detail is often distinctly different, pointing to asymmetric climate response between the two hemispheres rather than synchronicity. In opposite to other records found in the Northwest Pacific there is no sharp cooling spike around 8.2 kyr BP. Thus, New Zealand appears to be tied more closely to changes in circum-Antarctic and Southwest Pacific circulation than to events in the North-Atlantic.

Data from stalagmites in South Africa document climatic change in the Late Pleistocene and Holocene. A hiatus during the YD points to a pervasively dry and evaporative period, which was followed by a rather cool Mid-Holocene. In the late Holocene the features from other proxies, like for instance the Little Ice Age, are well visible [*Holmgren et al.*, 2003].

2.1.4 Marine evidence

2.1.4.1 Foraminifera-based proxies

DeMenocal et al. [2000] set up a faunal record of past SST variations in the subtropical Atlantic off the African coast based on isotope analyses in marine sediments. They pointed to a series of abrupt, millennial-scale cooling events, which punctuated the Holocene warm period and claimed these changes to be emerged from southward advection of cooler temperate or subpolar waters. Furthermore, they demonstrated that high- and low-latitude climates were coupled throughout the Holocene and that the timing of the subtropical Holocene cool events closely match those identified in the cores of Bond [1997; 2001].

A further marine sediment based, high-resolution proxy was introduced by Friddell et al. [2003]. The foraminiferal $\delta^{18}O$ record from the Santa Barbara Basin off the Californian coast revealed higher El Niño – Southern Oscillation (ENSO) activity during the warm phases of the Holocene and hence predicted increasing decadal- to centennial-scale climatic variability in the Pacific region.

A SST reconstruction for the northern Sargasso Sea in the Atlantic was presented by Keigwin [1996]. He analyzed the $\delta^{18}O$ in the sediments of surface-dwelling planktonic foraminifera from the Bermuda Rise, northern Sargasso Sea and revealed SST variations of about 1-2 K during the late Holocene events (MWP, LIA).

Stott et al. [2004] presented a SST reconstruction based on a combination of foraminiferal Mg/Ca and $\delta^{18}O$ measurements. The samples stemmed from four different cores in the western Pacific. Next to a slight decrease in SST and salinity during the past 10 kyr they found considerable variations in the late Holocene and suggested this variability to be linked with shifts in the position of the ITCZ.

2.1.4.2 Sea-bed sediments

Titanium and iron concentrations in marine sediments off the Venezuelan coast, which were stored in anoxic conditions of the Cariaco Basin, were used to derive the hydrological conditions in northern South America over the past 14 kyr with subdecadal resolution. They revealed a dry YD, followed by a period with increased precipitation during the Holocene optimum and drier conditions – however with high-amplitude fluctuations - in the late Holocene. The changes are supposed to be caused by regional shifts in the mean latitude of the ITCZ, potentially caused climate variability in the Pacific circulation patterns. Strong correlations with distant proxies point to global teleconnections, including the subsystem in the North Atlantic region [*Haug et al.*, 2001].

Lamy et al. [2006] investigated two sediment cores from the Anatolian continental slope in the southwestern Black Sea. They directly provide information about terrigeneous input from rivers in the Anatolian plain and are hence a proxy for the rainfall changes in this winter rain climate region, which is closely linked to the North Atlantic climate patterns.

Weijers et al. [2007] analyzed the characteristics of soil bacteria in a marine sediment record, which was recovered close to the Congo River outflow and reconstructed large-scale continental temperature changes in tropical Africa for the past 25 kyr. They observed that the temperature increase over the last glaciation is probably larger than previously thought.

2.1.5 Biological evidence

Subfossil remains of chironomids, a group of aquatic midges, have been used to reconstruct mean July paleotemperature in North Scandinavia by Laroque and Hall [2004]. The number of head capsules of the insects per volume of the sediment has been shown to be reliable for temperature reconstructions. The analyses showed that the temperatures steadily decreased after a recorded peak in the early Holocene about 9 kyr BP which fitted into different reconstructions based on other proxies in that area [*Larocque and Hall*, 2004 and references therein].

A further July mean air temperature reconstruction was presented by Seppa and Birks [2002]. They examined pollen sediments in Arctic lakes in terms of taxa and proportions. The main trends in July temperatures suggested a gradual early Holocene rise of summer temperatures and a gradual mid- and late-Holocene cooling with no explicit indications for rapid shifts.

Pollen-stratigraphical data from the Lake Flarken in south Sweden provided the basis for a 10 kyr proxy for annual mean temperatures [*Seppa et al.*, 2005]. The emerging relatively low temperatures in the early Holocene seemed to be in contrast to the comparably high insolation values. However, Seppa et al. claimed this fact to be triggered by the maritime climate, which

was influenced by stronger-than-present zonal flow in the North Atlantic. In the mid Holocene the thermal maximum of this record was reached followed by increasingly cold, moist and unstable climate.

Table 1: Information of the selected paleoclimatic proxy time series

No.	Location	Type and interpretation	Region	Author
1	Greenland	Ice core, $\delta^{18}O$, temperature	North Atlantic	[*Alley*, 2000]
2	Yukon	Lake sediment, $\delta^{18}O$, intensity and position of the aleutian high	North America	[*Anderson et al.*, 2005]
3	Norway	Morpho-stratigraphy, mean winter precipitation	North Atlantic	[*Bakke et al.*, 2005]
4	Israel, Soreq cave	Speleothem, $\delta^{18}O$ and $\delta^{13}C$, temperature and humidity	Africa	[*Bar-Matthews et al.*, 2003]
5	North Atlantic	Marine sediment, ice rafting	North Atlantic	[*Bond et al.*, 2001]
6	Brazil	Speleothem, $\delta^{18}O$, temperature	South America	[*Cruz et al.*, 2005]
7	Brazil	Speleothem, $\delta^{13}C$, humidity	South America	[*Cruz et al.*, 2005]
8	Subtropical Atlantic	Foraminiferal $\delta^{18}O$, SST, cool season	Africa	[*deMenocal et al.*, 2000]
9	Subtropical Atlantic	Foraminiferal $\delta^{18}O$, SST warm season	Africa	[*deMenocal et al.*, 2000]
10	Dongge, China	Speleothem, $\delta^{18}O$, temperature	West Pacific	[*Dykoski et al.*, 2005]
11	Epica Dome L	Ice core, $\delta^{18}O$, temperature	Antarctica	[*EPICA and Members*, 2007]
12	Qunf Cave, Yemen	Speleothem, $\delta^{18}O$, precipitation	Africa, Low Latitudes	[*Fleitmann et al.*, 2007]
13	Santa Barbara Basin	Marine sediment, $\delta^{18}O$, temperature	North America	[*Friddell et al.*, 2003]
14	Cariaco Basin	Titanium traces, humidity	South America, Low Latitudes	[*Haug et al.*, 2001]
15	South Africa	Speleothem, $\delta^{18}O$ and $\delta^{13}C$, temperature and humidity	Africa	[*Holmgren et al.*, 2003]
16	Epica Dome C	Ice core, $\delta^{18}O$, temperature	Antarctica	[*Jouzel et al.*, 2001]
17	Sargasso Sea	Foraminifera, $\delta^{18}O$, SST	North Atlantic	[*Keigwin*, 1996]
18	Great Plains, USA	Lake sediment, evaporation / temperature	North America	[*Laird et al.*, 1996]

19	Gulf of Aqaba	Marine sediment, $\delta^{18}O$, SST	Africa	[*Lamy et al.*, 2006]
20	Abisko, Sweden	Pollen, temperature	North Atlantic	[*Larocque and Hall*, 2004]
21	Cariaco Basin	Mg/Ca, SST	South America, Low Latitudes	[*Lea et al.*, 2003]
22	Antarctica	Ice core, d D, temperature	Antarctica	[*Petit et al.*, 1999]
23	Finnland	Pollen, July mean temperature	North Atlantic	[*Seppa and Birks*, 2002]
24	Sweden	Pollen, annual mean temperature	North Atlantic	[*Seppa et al.*, 2005]
25	Taylor Dome	Ice core, $\delta^{18}O$, temperature	Antarctica	[*Steig et al.*, 1998]
26	Taylor Dome	Ice core, δD, temperature	Antarctica	[*Steig et al.*, 1998]
27	Western Pacific	Foraminifera, SST	West Pacific, Low Latitudes	[*Stott et al.*, 2004]
28	Greenland	Ice core, $\delta^{18}O$, temperature	North Atlantic	[*Stuiver et al.*, 1995]
29	Kilimanjaro	Ice core, $\delta^{18}O$, temperature	Africa, Low Latitudes	[*Thompson et al.*, 2002]
30	Nevado Huascaran, Peru	Ice core, $\delta^{18}O$, temperature	South America, Low Latitudes	[*Thompson et al.*, 1995]
31	Sajama Mountains, Bolivia	Ice core, $\delta^{18}O$, temperature	South America, Low Latitudes	[*Thompson et al.*, 1998]
32	North America	Pollen, temperature	North America	[*Viau et al.*, 2006]
33	Greenland, GRIP	Ice core, $\delta^{18}O$, temperature	North Atlantic	[*Vinther et al.*, 2006]
34	Greenland, NGRIP	Ice core, $\delta^{18}O$, temperature	North Atlantic	[*Vinther et al.*, 2006]
35	Dongge, China	Speleothem, $\delta^{18}O$, Strength of the East Asian Monsoon	West Pacific	[*Wang et al.*, 2005]
36	Congo estuary	Soil bacteria in marine sediments, temperature	Africa, Low Latitudes	[*Weijers et al.*, 2007]
37	New Zealand, South Island	Speleothem, $\delta^{18}O$, temperature	West Pacific	[*Williams et al.*, 2005]
38	New Zealand, North Island	Speleothem, $\delta^{18}O$, temperature	West Pacific	[*Williams et al.*, 2004]
39	Lake Huguang, China	Magnetic susceptibility, strength of the winter monsoon	West Pacific	[*Yancheva et al.*, 2007]
40	Lake Huguang, China	Ti count, position of the ITCZ	West Pacific	[*Yancheva et al.*, 2007]

3 Methods

3.1 Data preparation

3.1.1 Time series synchronization and harmonization

Before comparing the manifold proxy series, we harmonized the timescales to the unit kiloyear before present (kyr BP), where present commonly relates to the year 1950. In certain cases the values therefore became negative, since the time series last to years later than 1950 AD.

The two methods applied in this thesis both require equal temporal resolution in order to derive comparable results. To achieve this, the time series were low pass filtered with a method comparable to the running mean. A given resolution was defined before filtering the data. In our case, we low-pass filtered the data with 200-year mean values. The predefined timescale hence had a 200-year resolution. Subsequently, the values ± 100 cal years were averaged for each predefined point on the timescale, resulting in a smoothed time-series with a comparable temporal resolution.

3.1.2 Detrending

Detrending describes the substraction of values, which are computed with fitting models, of the non-detrended time series. Trends in time series can hence be removed with using linear, exponential or spline models. Since change-point analysis aims to detect the significant phases of time series, including transitions from more or less stable phases to phases with clear trends, the time series were not detrended in order not to loose any information about changes. For the same reason the time-series prior to the detection of rapid climate change was not detrended either.

3.2 Changepoint analysis

3.2.1 A test for a change point based on cumulative sums

The procedure to detect change points used in this thesis is based on a combination of cumulative sum charts (CUSUM) and bootstrapping as proposed by Taylor [2000]. This approach is easily adaptable to the task of this thesis as well as simple to compute in the program environment used.

CUSUM was first introduced by Page [1954] and further established by Hinkley [1971]. Taylor [2000] presented a step by step computational solution for this approach.

The analysis begins with the calculation of cumulative sums S_i for each time step calculated as follows: $S_i = S_{i-1} + (X_i - \overline{X})$, where $\overline{X}$ is the average of the sample time series and $S_0 = 0$.

This series is plotted in figure 7 (b) as the black curve. By definition it starts and ends at zero. Suppose that during a period of time the values tend to be below the overall average. The S_i values will be negative and the sum will steadily decrease. In our example this is clearly visible in the time span from 0 – 5 kyr BP. Likewise a segment with upward slope indicates a period with values higher than the overall average. A sudden change in the direction of the CUSUM values indicates a shift or change in the average. Periods of stable values are shown in horizontal paths on the CUSUM chart.

The black curve in figure 7 (b) depicts a clearly visible change 5 kyr BP and minor turnarounds at 2.6, 6.2 and 9 kyr BP.

3.2.2 Test of significance based on bootstrapping

The significance of the presumed change point at 5 kyr BP can be determined by assessing a confidence level based on bootstrapping. Hence iterative steps approximate the solution, each of it leading closer to an analytical solution.

As a check value to be compared with the bootstraps, an estimator of the magnitude of change is defined by computing the difference between the largest and lowest CUSUM value: $S_{diff} = S_{\max} - S_{\min}$

In the consecutive step, reordering the original time series values in random order generates the first bootstrap sample. This process is generally called sampling without replacement. CUSUM values and the S_{diff} value are subsequently calculated for this bootstrap in the same way it was for the original time series. The final step of each bootstrap is to compare the derived S_{diff} with the original one. The idea behind this approach is to imitate the CUSUM values when no changes occur. With a large number of bootstraps numerous S_{diff} values are created and the comparison of the original S_{diff} with the variation of the bootstrapped values give an indication about the significance of the change. Let N be the number of bootstraps and X the number of bootstrapped S_{diff} values, which are larger than the original S_{diff}, then the confidence level is calculated as followed:

$$ConfidenceLevel = 100 \cdot \frac{X}{N} \%$$

A clear picture of a high significance emerges in the example in Figure 7 (b). After six bootstraps the original S_{diff} remains still the highest peak. Even after 1000 iterations a significance of 100% was found for the first change point at 5 kyr BP.

Finding further change points is performed by analyzing the fragments between the beginning of the time series, the change points and the end of the time series until there is no

significance left. The final analysis of our sample dataset showed a further significant change point at 2.6 kyr BP. 951 of 1000 bootstraps showed a smaller S_{diff} value. The change point is hence only weakly significant. The two supposed change points at 6.2 and 9 kyr BP emerged not to be significant.

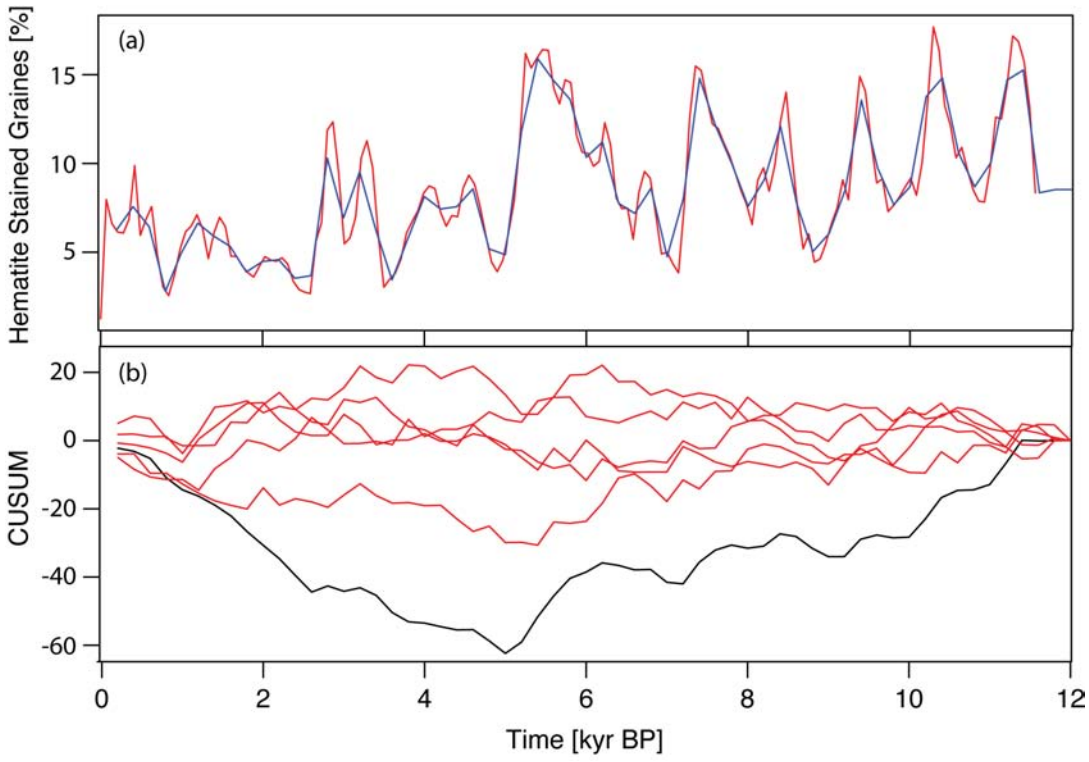

Figure 7: (a) Time series synchronization using the example of Bond [2001] and (b) CUSUM-bootstrapping.

3.3 Detecting of rapid climate change using regression

In order to detect the phases of rapid climate change, a simple and straightforward method was applied assuming that the change in a climate parameter is rapid, if the response in the proxy is strong as well.

Analogously to the synchronization of the time series resolution (see chapter 3.1.1), a resolution of 200 years for the analyses was predefined. For each time step, a temporal window of 200 cal yrs was used to define values for a linear regression. Hence for the 0.4 kyr BP-step for instance, a linear regression with the values from 0.3 – 0.5 kyr BP was computed. The slope of the linear equation resulting from the regression is thus a measure for the gradient of change during this time period. In the following, the fraction with the strongest gradients of each time series was marked. In our survey, 20% were marked, although other

authors described a higher fraction of the Holocene to be a phase of rapid climate change. Mayewski [2004] for instance proposed 35% of the past 11.5 kyr to be a phase of rapid climate change.

3.3.1 Test of significance based on calculus of probability

The calculation how many k = time series with a strong gradient at the same time are necessary for hitting the level of significance is a matter of calculus of probability. For simplicity, we reverse the question about the significance into the following: How high is the probability p that k members of n random time series show a increased gradient at a specific time, when 20% of each time series is marked as rapid climate change?

Obviously, the chance that k=1 strong gradient is marked at a random point in time is p=0.2 for n=1, and p=0.2 · 0.8 for n=2.

Expanding to more time series however is not straightforward and we assume n=7 and k=[0,7] as an example for deducing a general formula to compute the probabilities $p_{[0,7]}$ for 0 to 7 members.

The probability p_0 that none of the time series n is marked, therefore k=0, is obviously $p_0=0.8^7$ and analogously $p_7=0.2^7$. The probability for k=[1,6] is – expressed in words – the probability that a certain arrangement of marked members occurs times the number of possible combinations of members. If we therefore want to know the probability p_4 that four members show increased gradients at the same time, the probability that a specified group of four is $p=0.8^4 \cdot 0.2^3$ and the number of possible combinations of groups with four members is $\binom{n}{k} = \frac{n!}{k!(n-k)!} = \frac{7!}{4!(7-4)!} = 35$. The probability that four members of a population of seven random time series show a strong gradient is hence $p_4=35 \cdot 0.2^4 \cdot 0.8^3=0.029$. In other words: if four of seven time series in our diagrams show an increased gradient at the same time, the probability is only 2.9% that this is a random occurrence. Assuming a level of significance of 95% we can state this as a significant indication of a forced change.

Table 2: Probabilities for n=7

k	*Combinations*	*Formula*	$p_{[0,7]}$
0	1	$1 \cdot 0.8^7$	0.21
1	7	$7 \cdot 0.2^1 \cdot 0.8^6$	0.37
2	21	$21 \cdot 0.2^2 \cdot 0.8^5$	0.28
3	35	$35 \cdot 0.2^3 \cdot 0.8^4$	0.11
4	35	$35 \cdot 0.2^4 \cdot 0.8^3$	$2.86 \cdot 10^{-2}$
5	21	$21 \cdot 0.2^5 \cdot 0.8^2$	$4.30 \cdot 10^{-3}$
6	7	$7 \cdot 0.2^6 \cdot 0.8^1$	$3.58 \cdot 10^{-4}$
7	1	$1 \cdot 0.2^7$	$1.28 \cdot 10^{-5}$

4 Results

This chapter discusses the results of the change-point analyses (chapter 3.2) and the detection of RCC (chapter 3.3) carried out on the proxy dataset introduced in chapter 2.

4.1 Change point analysis

The following graphs are all designed identically. A red curve always represents a primarily temperature-sensitive proxy, a blue time series indicates a humidity- or precipitation-driven proxy whereas a black curve shows a further climatic factor, like for instance the meridional position of the ITCZ. In order to estimate the variability during the significant phases, the mean and the standard deviation is depicted with a green and two black lines.

4.1.1 Africa

The eight proxies for the African continent (figure 8) mainly show paleotemperatures. Only the speleothem proxy on the Arabian Peninsula is sensitive to humidity. The speleothem of South Africa and the marine sediment in the Gulf of Aqaba show no significant change point. The other proxies show five phases of grouped change points about 10, 8.2, 7, 6.4 and 5.6 kyr BP. The late Holocene shows stable conditions, there is only one change point in the Qunf cave speleothem proxy. This one however is caused by a discontinuity in the time series.

The 10 kyr BP change points indicate a beginning phase of warmer and dryer conditions, registered in the proxies in the Congo delta and in Yemen. The second peak around 8.2 kyr BP was significantly registered on the Arabian Peninsula in the subtropical Atlantic with slightly decreasing air temperatures and SST. The Congo estuary however shows increasing temperature at this time. The group of change points around 8.2 kyr BP is likely triggered by a catastrophic outburst from Lake Agassiz through the Hudson strait into the Northern Atlantic, causing a massive change in oceanic and atmospheric circulation over the North Atlantic [*Alley et al.*, 1997; *Alley and Agustsdottir*, 2005]. Our set of proxies indicates that those, who showed a decrease in temperature after this event both revealed a significant recover about 1.2 kyr later. The following change shows tendencies to the opposite direction. The temperature-sensitive isotope proxy on the Kilimanjaro indicates a lowering of the temperature, whereas in the congo estuary the air temperature increases. The last heavy alteration occurred about 5.6 kyr BP, when the record on the Kilimanjaro and the SST reconstructions for the subtropical Atlantic showed higher temperatures, connected with higher humidity in the Qunf cave record.

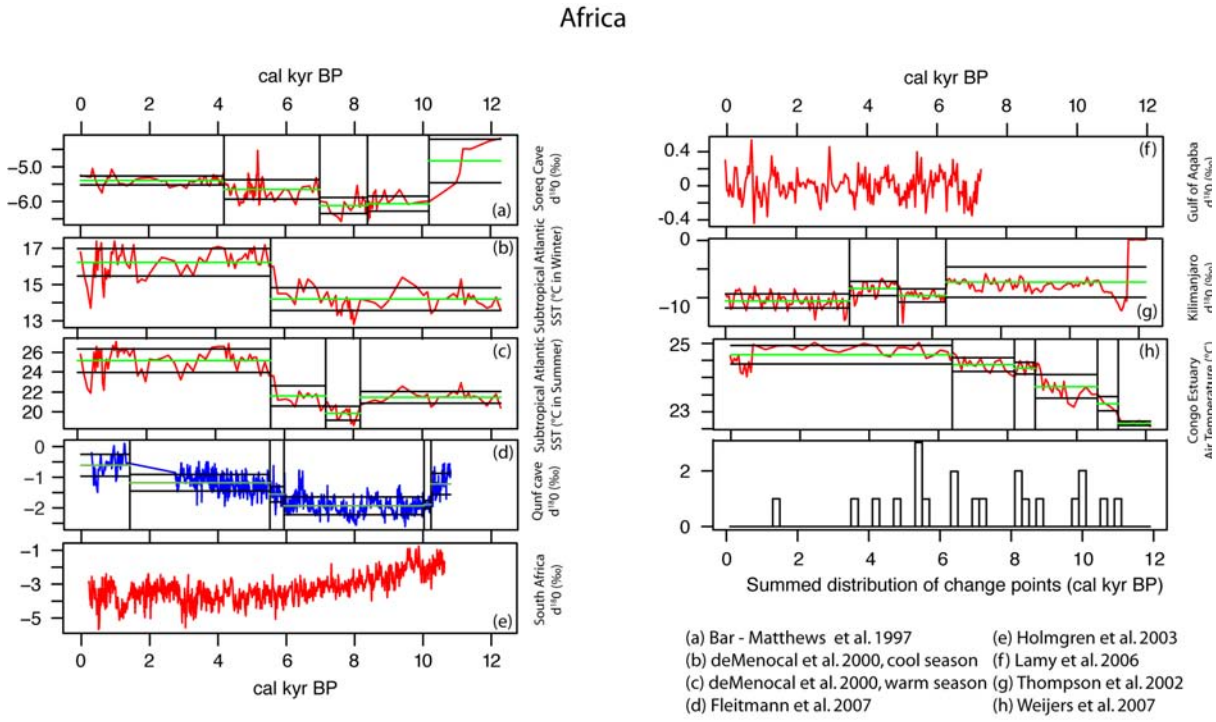

Figure 8: Change point analysis for the selected proxies in the African region.

4.1.2 Antarctica

The five proxy archives from Antarctica (figure 9) only represent temperature. The ice cores from the EPICA project and from Vostok, both in West Antarctica, clearly show the warming coinciding with the termination of the YD. A distinct scheme in the changes is not visible in the first half of the Holocene. A peak around 2.4 kyr BP, which is depicted in four of the five proxies and shows a lowering of the δ18O, dominates the last 6 kyr BP. The rest of the second half of the Holocene tends to be more stable than the first 6 kyr.

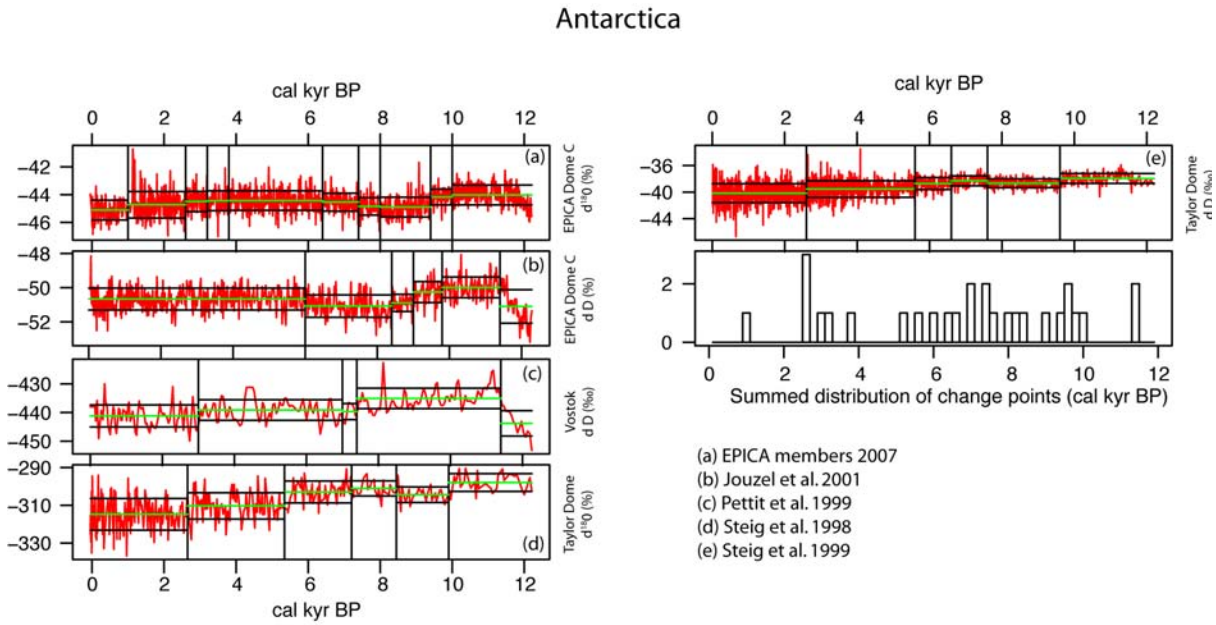

Figure 9: Change point analysis for the selected proxies in Antarctica.

4.1.3 Low latitudes

The summarized tropic proxies (figure 10) show an ambiguous picture. The only obvious alteration emerges at 6.4 kyr BP. As mentioned in chapter 4.1.1 the African temperature proxies are going in the opposite direction. The humidity in the Cariaco Basin shows a decrease at this time and the South American proxy of the Nevado Huascaran indicates slightly lower temperatures.

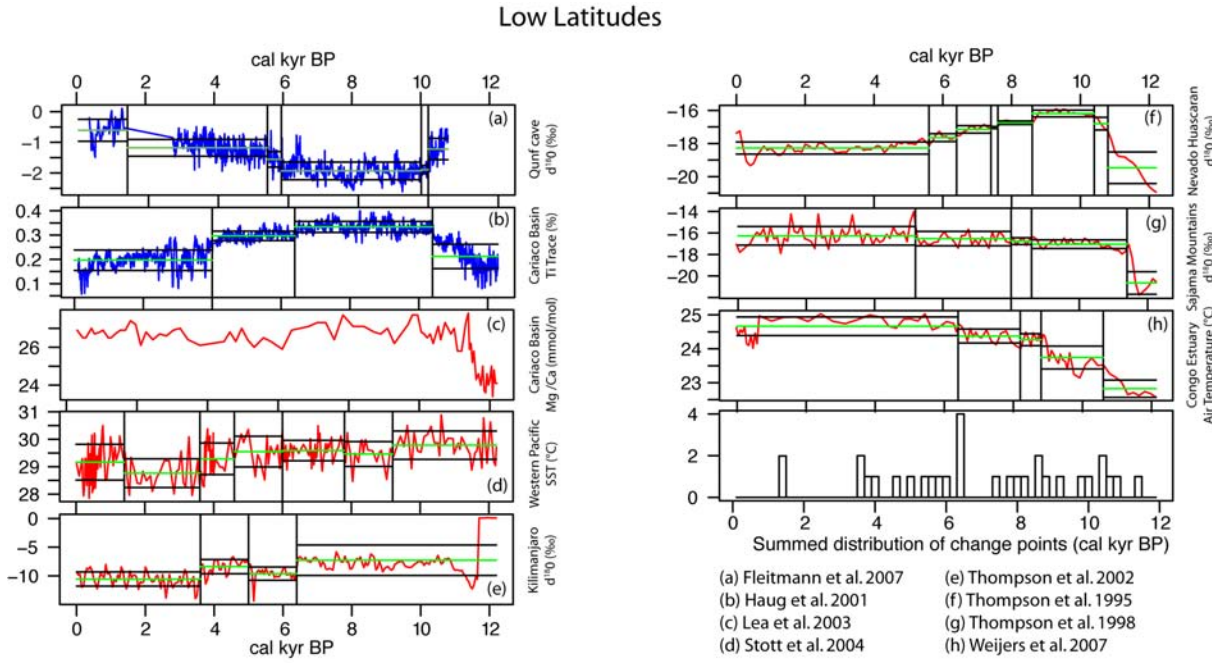

Figure 10: Change point analysis for the selected proxies in the Low Latitudes.

4.1.4 North America

As the only proxy covering the entire Holocene, the temperature reconstruction by Viau et al. [2006] shows the transfer from the YD to the Holocene by rising temperatures, which are reflected in three significant change points in the first 3 kyr of the Holocene (figure 11). The temperatures in the Santa Barbara Basin indicate at the same time a decrease. Further changes have happened in the time around 7.5 kyr and 2.8 kyr BP, where the latter indicates the beginning of a phase with slightly lower temperatures and a strengthened Aleutian low.

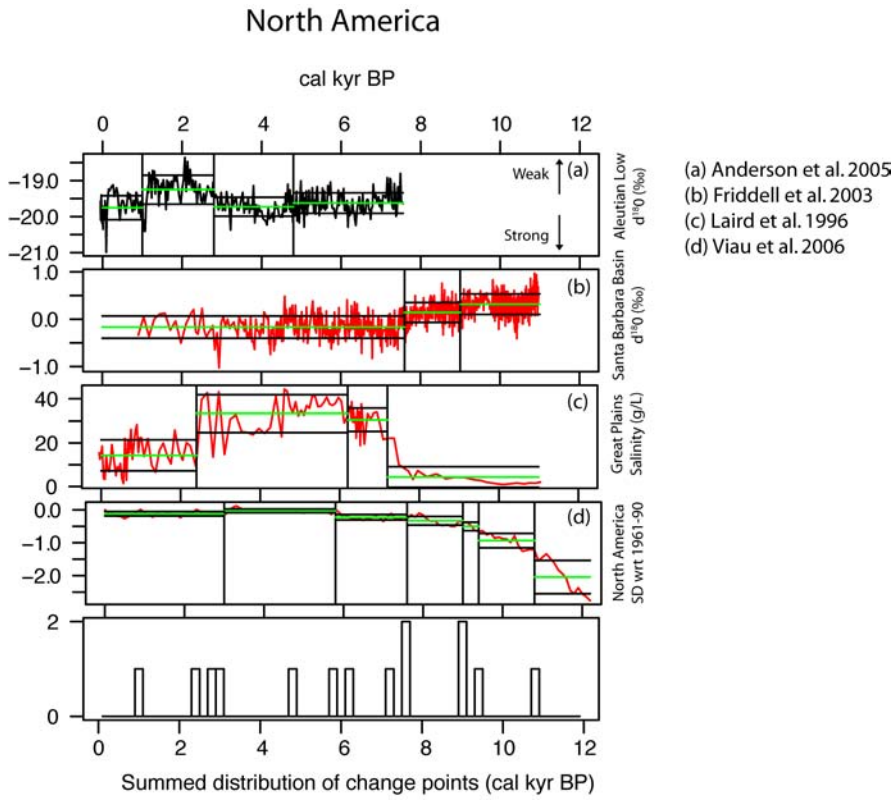

Figure 11: Change point analysis for the North American proxies.

4.1.5 North Atlantic

The most obvious sum of change points in the North Atlantic region coincides with the transition from the YD to the Preboreal about 11.4 kyr BP (figure 12). The entire ice core based temperature-sensitive proxy set from Greenland show this change point. This set furthermore shows an aggregation around 10 kyr BP towards higher $\delta^{18}O$ values.

The concentration around 8.2 kyr BP depicts higher temperatures in Finland and in one of the Greenland proxies. The temperature in the Sargasso Sea tends to lower, however with an increasing variability. These results differ from the expectations based on the idea of a large-

scale cooling emerged from the Lake Agassiz outbreak [*Alley et al.*, 1997; *Alley and Agustsdottir*, 2005]. Change points around 5 kyr BP show lowered temperatures in one Greenland proxy and both of the Scandinavian air temperature reconstructions. At the same time, ice rafting in the North Atlantic reaches a weak phase. The most recent cluster occurred at 2 kyr BP and showed a starting phase of lower temperatures in the Greenland ice cores and the summer temperatures of South Sweden.

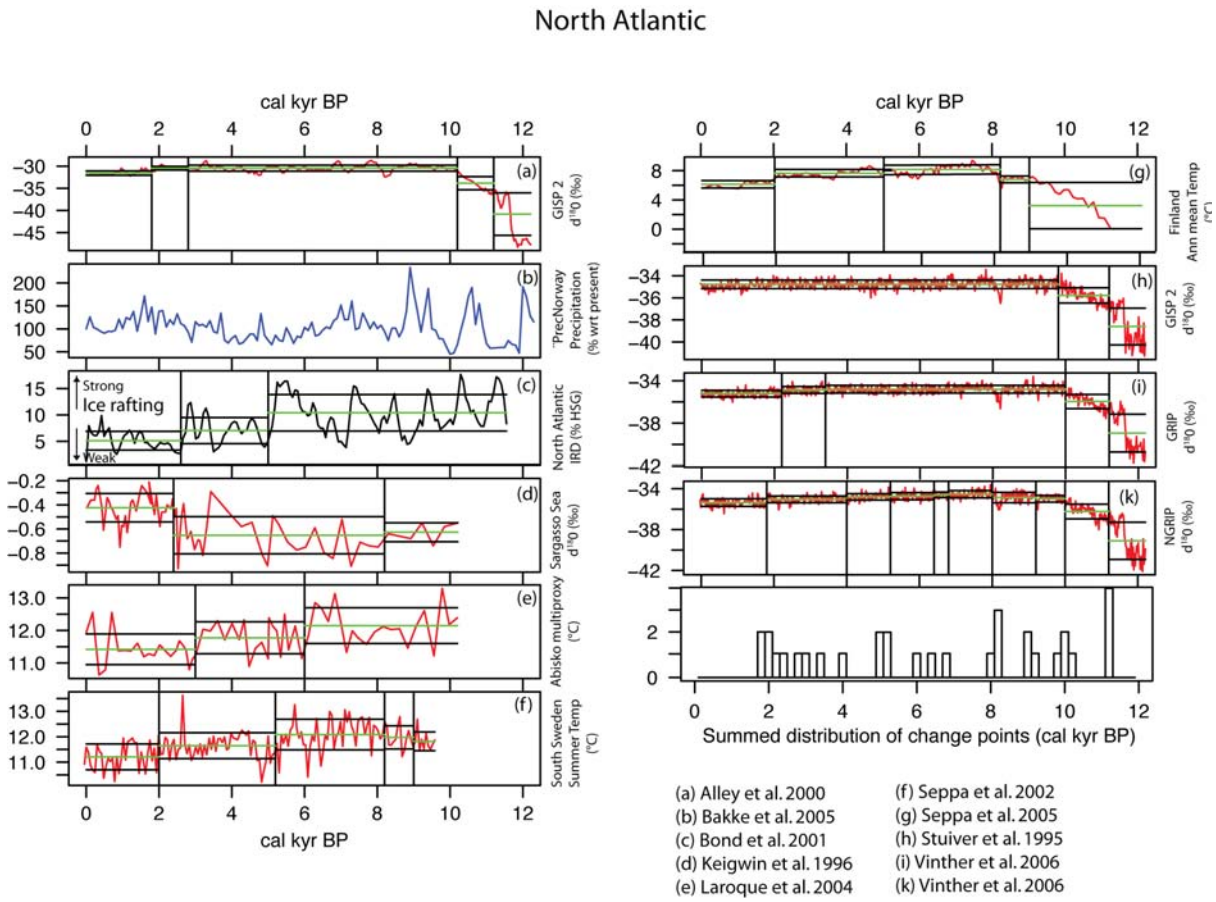

Figure 12: Change point analysis for the North Atlantic proxies.

4.1.6 South America

The South American proxies show an indistinct scheme of change points (figure 13). A weak clustering around 10.2 kyr BP denotes the beginning of a warmer and rather moist phase all over the continent. This period ends at 6.4 kyr BP and in the consecutive centuries. The humidity sensitive proxies show afterwards rather dry conditions, whereas two proxies responding to temperature show decreasing and the other two increasing temperature.

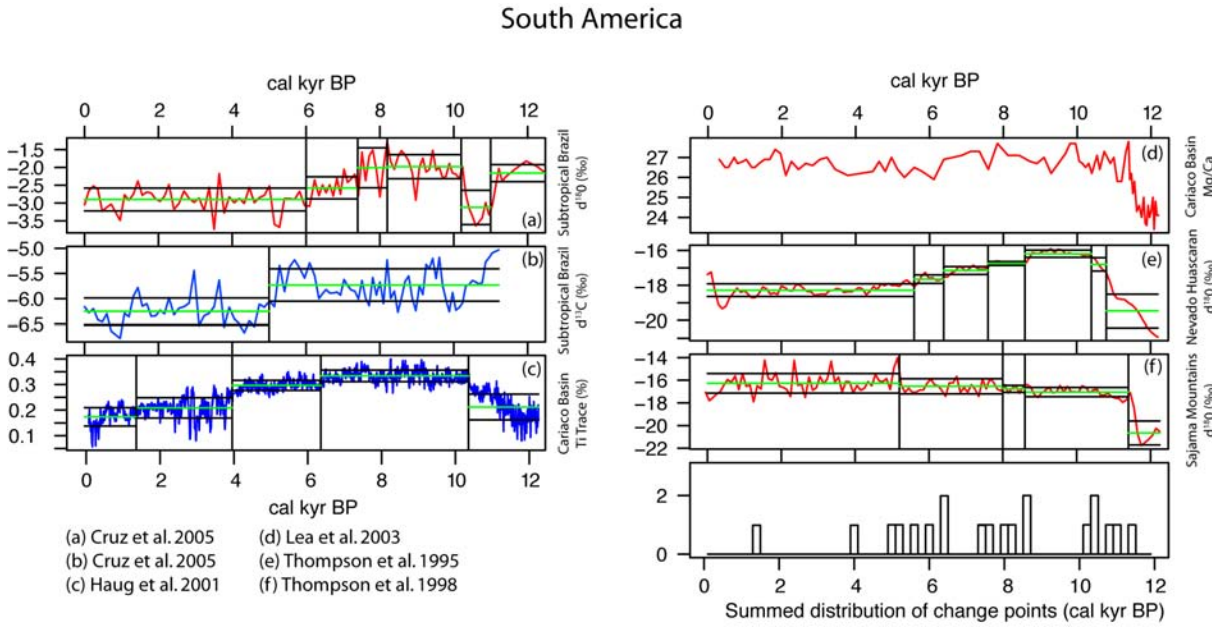

Figure 13: Change point analysis for the South American proxies.

4.1.7 West Pacific

The early Holocene of the West Pacific region is characterized by only a few significant changes (figure 14). A first eye-catching summation of change points occurred around 7.8 kyr BP. The Winter Monsoon lost intensity and at the same time the ITCZ started to move northward. The temperature responding proxy in the Dongge Cave and the SST reconstruction show a slight rise. Furthermore, a cluster occurs at 4.6 kyr BP. However, it does not show a consistent picture. Winter Monsoon slightly gained intensity. The Dongge cave proxies point to a warming, whereas the West Pacific SST tended to decrease.

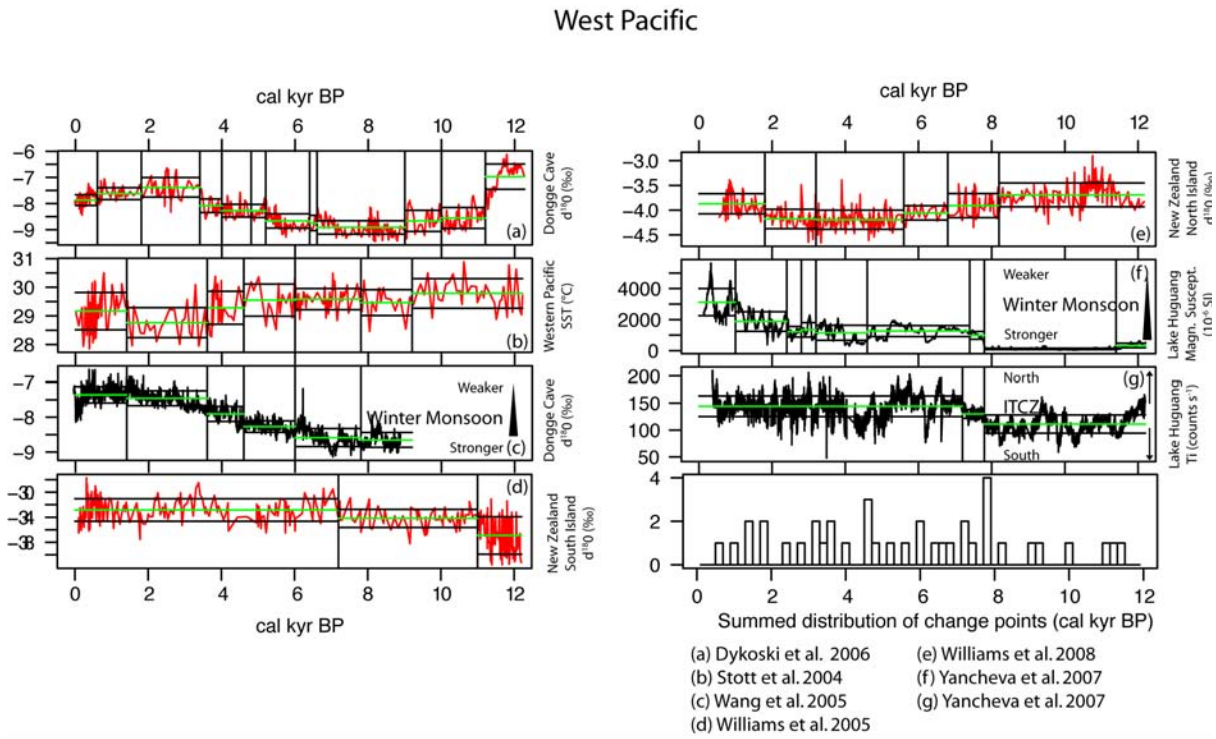

Figure 14: Change point analysis for the West Pacific proxies.

4.2 Detection of rapid climate change

Analogously to the plots for the change point analysis (chapter 4.1) the proxy series' colors display the nature of the proxy; red depicts temperature-sensitivity, blue humidity and black another characteristic climate parameter. As some of the time series did not cover the entire Holocene, we were forced to skip these datasets and the number of proxies hence decreased. As in the previous chapter, the results were regionally summed and depicted in a histogram. The level of significance, as defined in chapter 3.3.1, was marked with a red line in the cases, where the significance was hit.

4.2.1 Africa

In Africa, the level of significance was hit during two periods throughout the Holocene (figure 15). In the first event 6.4 kyr BP three of the proxies indicated a RCC towards lower temperatures. The second event with a significant number of RCC indications took place in the very last centuries of the Holocene from 0.7 – 0.1 kyr BP. From 0.7 – 0.5 kyr SST and the air temperature sensitive proxies rapidly decreased, followed by an inconsistent phase of increasing SST in the subtropical Atlantic and rising $\delta^{18}O$ values in the Soreq Cave – proxy and the Kilimanjaro Ice Core, and rising temperature in the Congo estuary. Further peaks emerged at 1.8 and 3.6 kyr BP, both with indications of rapidly dropping temperature.

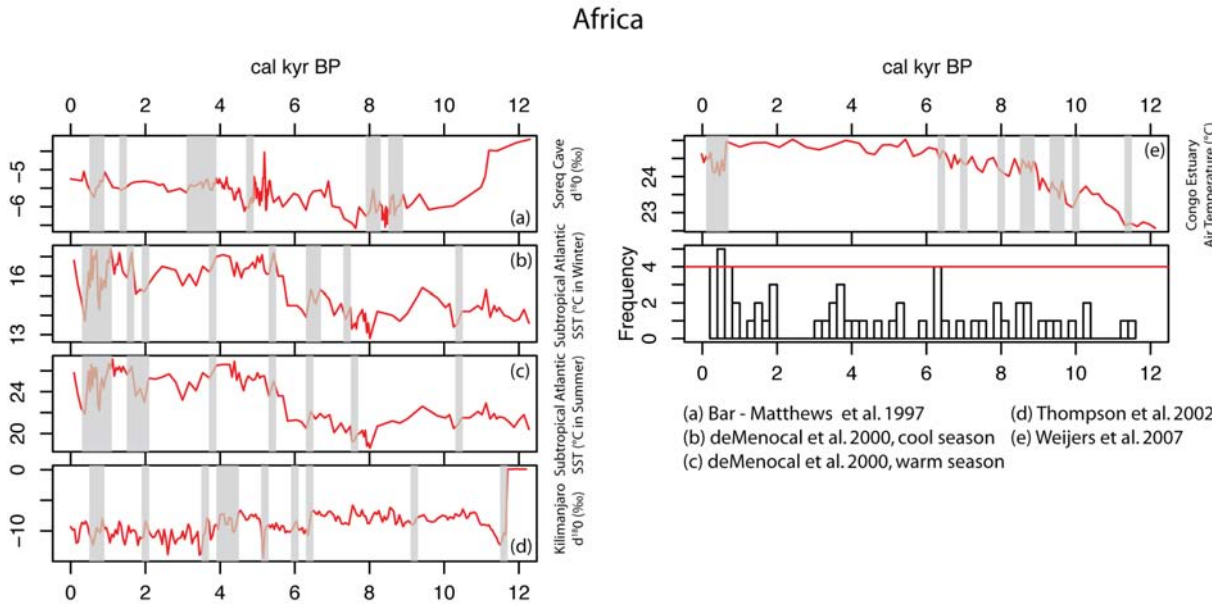

Figure 15: Detection of rapid climate change in African proxies.

4.2.2 Antarctica

The five high-resolution proxies of the Antarctica did not hit the level of significant rapid climate change in the Holocene (figure 16). However, there are a few culminations to consider. The first and – including the adjacent centuries – most striking one was 6.4 kyr BP. It shows a decrease in all of the temperature sensitive proxies. Another close to significant occurrence happened 4 kyr BP, also showing a rapid decrease in temperature. The 2.6 kyr BP cluster shows a rapid decrease as well.

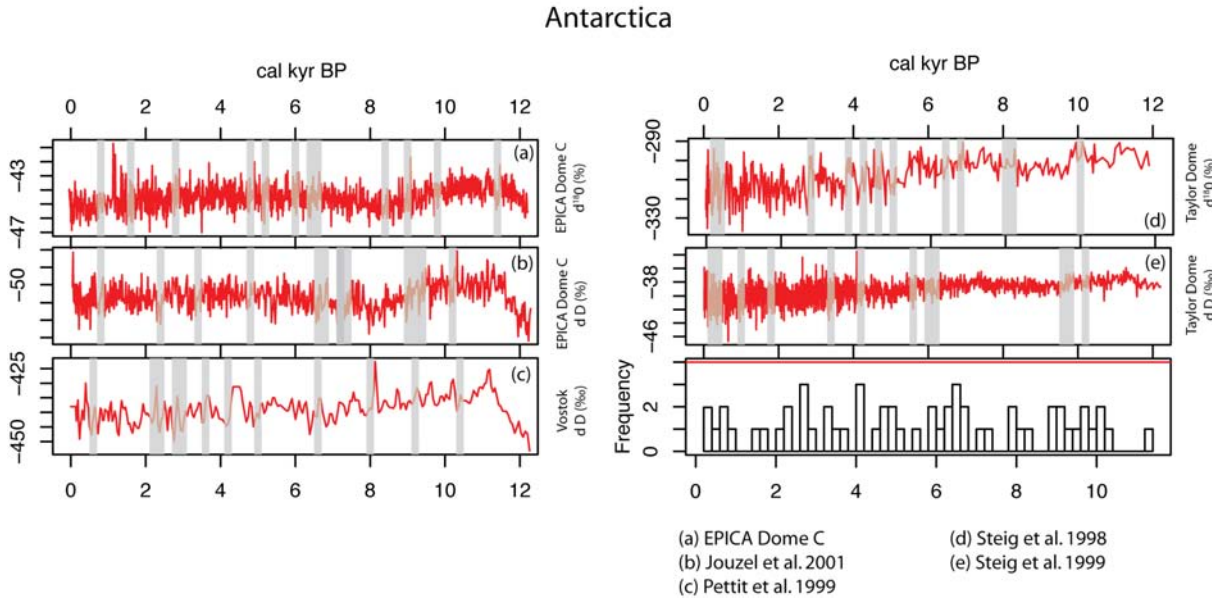

Figure 16: Detection of rapid climate change in the Antarctic proxies.

4.2.3 Low latitudes

In the Tropics, the level of significance was hit once during the entire Holocene (figure 17). Around 3 kyr BP the Kilimanjaro and the Western Pacific SST reconstruction show a cold relapse, however only of short duration. The proxy in the Nevado Huascaran and the Sajama mountains only changed a little towards cooler temperatures.

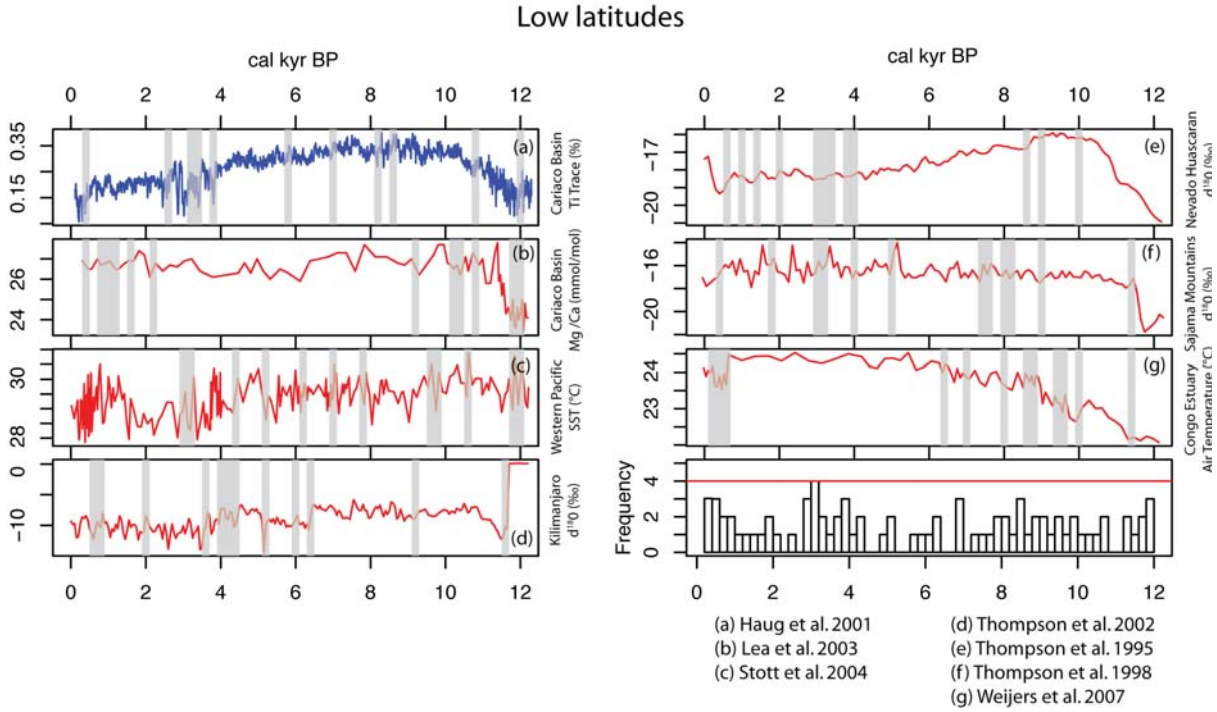

Figure 17: Detection of rapid climate change in the Low Latitudes.

4.2.4 North America

Due to its small number of samples of only two, a significant indication of RCC could not be reached (figure 18). However, there are two phases with common indications to RCC. Around 3.2 kyr BP and 0.6 kyr BP a cold snap was registered in both of the temperature sensitive proxies.

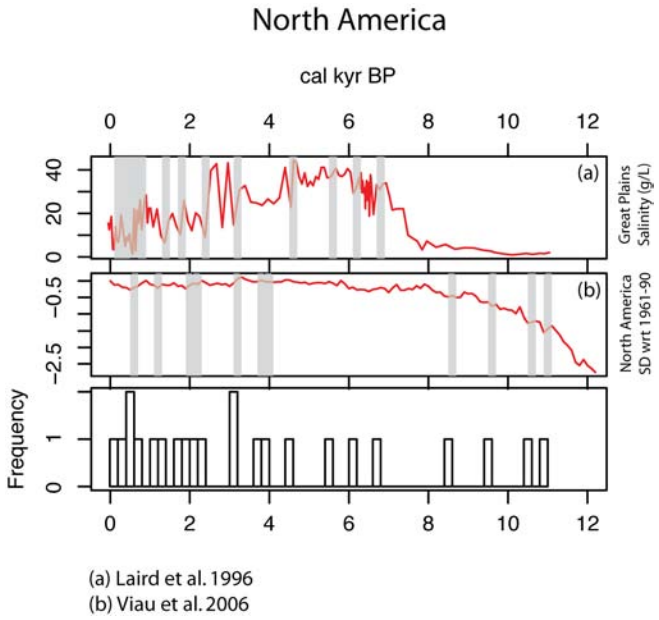

Figure 18: Detection of rapid climate change for the North American proxies.

4.2.5 North Atlantic

The level of significance of four proxies showing RCC was not hit in the set of the North Atlantic proxies (figure 19). There are however several attention-grabbing summations throughout the Holocene starting at 10.2 kyr BP with a cold relapse which is recorded in two Greenland ice cores and a rapid decrease in the precipitation in Norway. This phase corresponds with the one of the peaks in Bond's ice rafting data. The following peak coincides well with the Lake Agassiz outbreak 8.2 kyr BP and indicates the same rapid changes as in the first event, hence a cooling in the ice core proxies and a lower precipitation in Norway. 0.2 kyr later, two more proxies depict a phase of strong change.

The following peaks all indicate the same pattern of rapid climate change. Temperature signals in the ice core based proxies point to a decrease whereas the precipitation sensitive proxy from Norway shows less precipitation. The peaks occur at 7.6, 6.6, 5.2, 3 and 1.8 kyr BP.

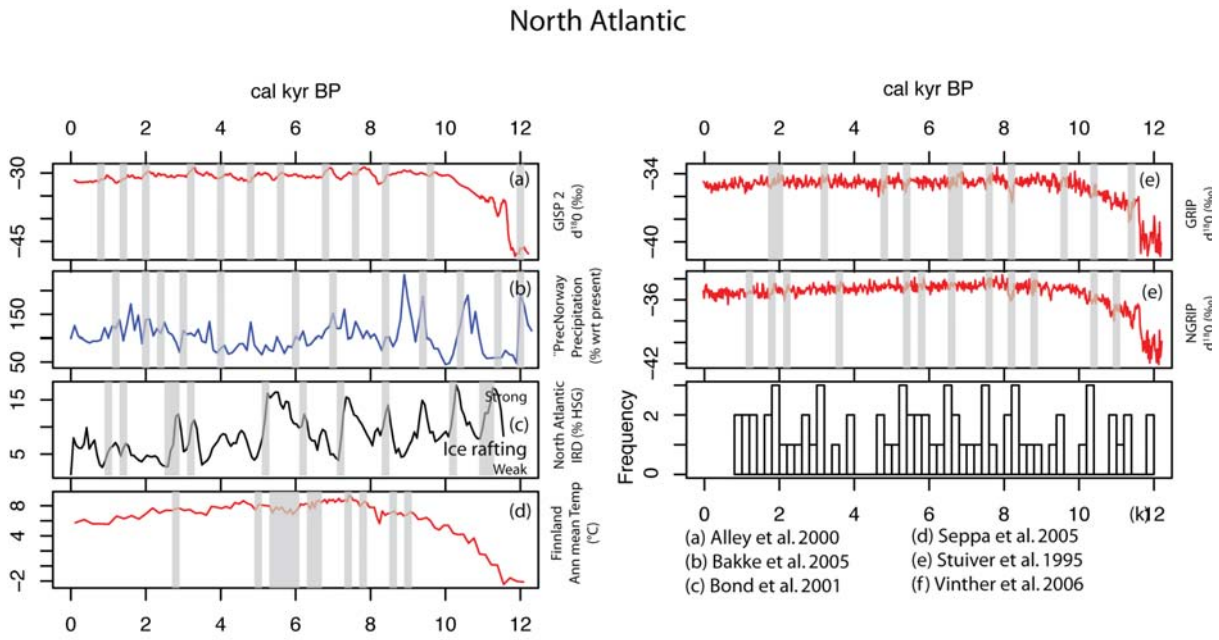

Figure 19: Detection of rapid climate change for the North Atlantic proxies.

4.2.6 South America

Several eye-catching clusters dominate the summation of the South American proxies (figure 20). The level of significance was hit two times in the early Holocene and once in the past 1000 years. The first event was 10.6 kyr BP and points to colder and dryer conditions unless in the very North of the continent. A further RCC event occurred around 8.8 kyr BP. Most of the proxies then showed a cooling and drying event, the Cariaco Basin however points to increasing temperature at that point. The events in the late Holocene took place at 0.8 and 0.4 kyr BP. The Cariaco Basin and the Subtropical Brazil show increasing temperature and decreasing humidity, whereas the proxy in the Nevado Huascaran indicates colder conditions.

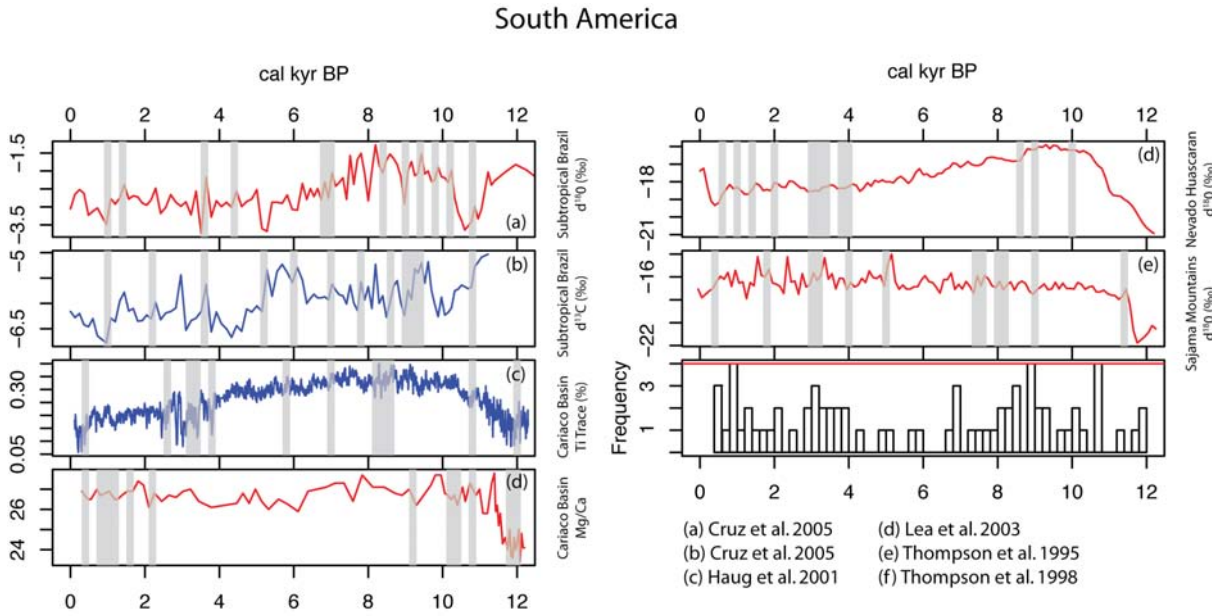

Figure 20: Detection of rapid climate change for the South American proxies.

4.2.7 West Pacific

The level of significance – four proxies indicating RCC at the same time – was not hit in the West Pacific proxy set (figure 21). However, some considerable clusters appear throughout the entire Holocene. The first summation appears at 11.8 kyr BP, when changes in the intensity of the Monsoon and the position of the ITCZ coincide with a period of high variability in the Western Pacific SST. A southward move of the ITCZ at 10.2 kyr BP coincides with the cooling in the New Zealand region and a decrease in the Dongge Cave. The strongest summation appears around 2.9 kyr BP. The ITCZ was then moving southward and the Winter Monsoon weakened after a first strengthening. The temperature was once more influenced by a cold relapse.

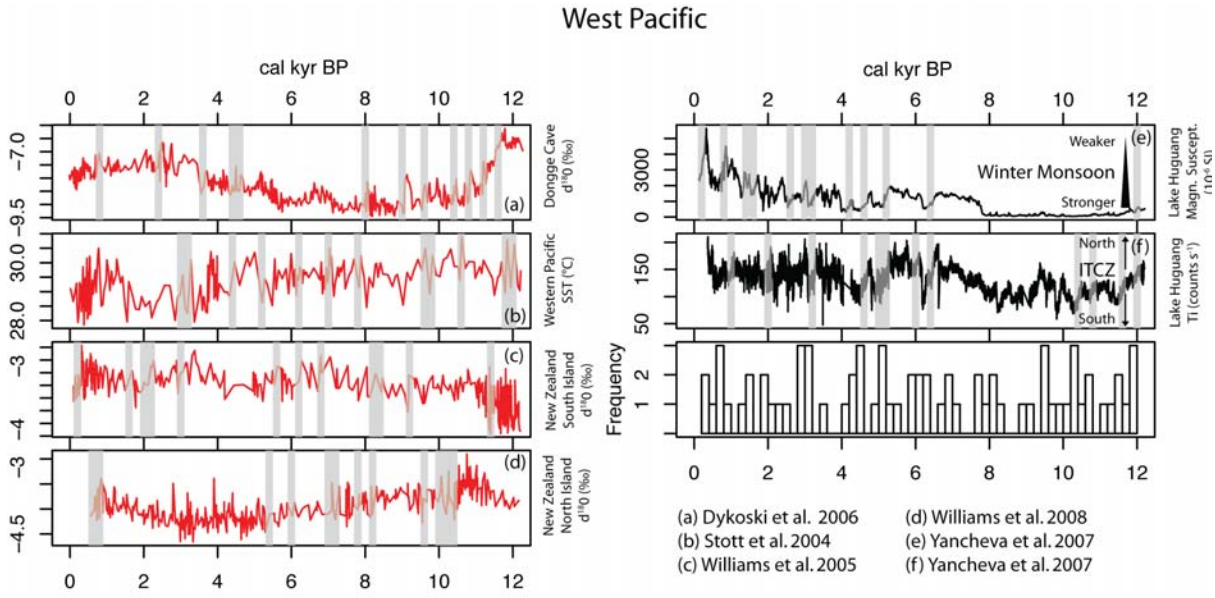

Figure 21: Detection of rapid climate change for the West Pacific proxies.

4.3 A global synopsis of RCC and change point analysis

Figure 22 depicts all the aforementioned change points and RCC indications regionally subdivided and with a brief hint to the direction of the change. Noticeable clusters of change over all regions are apparent around 2.8 and 6.4 kyr BP. A furthermore considerable aspect are the quasi-periodic occurrences in the North Atlantic, which correspond well with the idea of a cyclic behavior and their underlying IRD records as demonstrated by Bond et al. [1997; 2001].

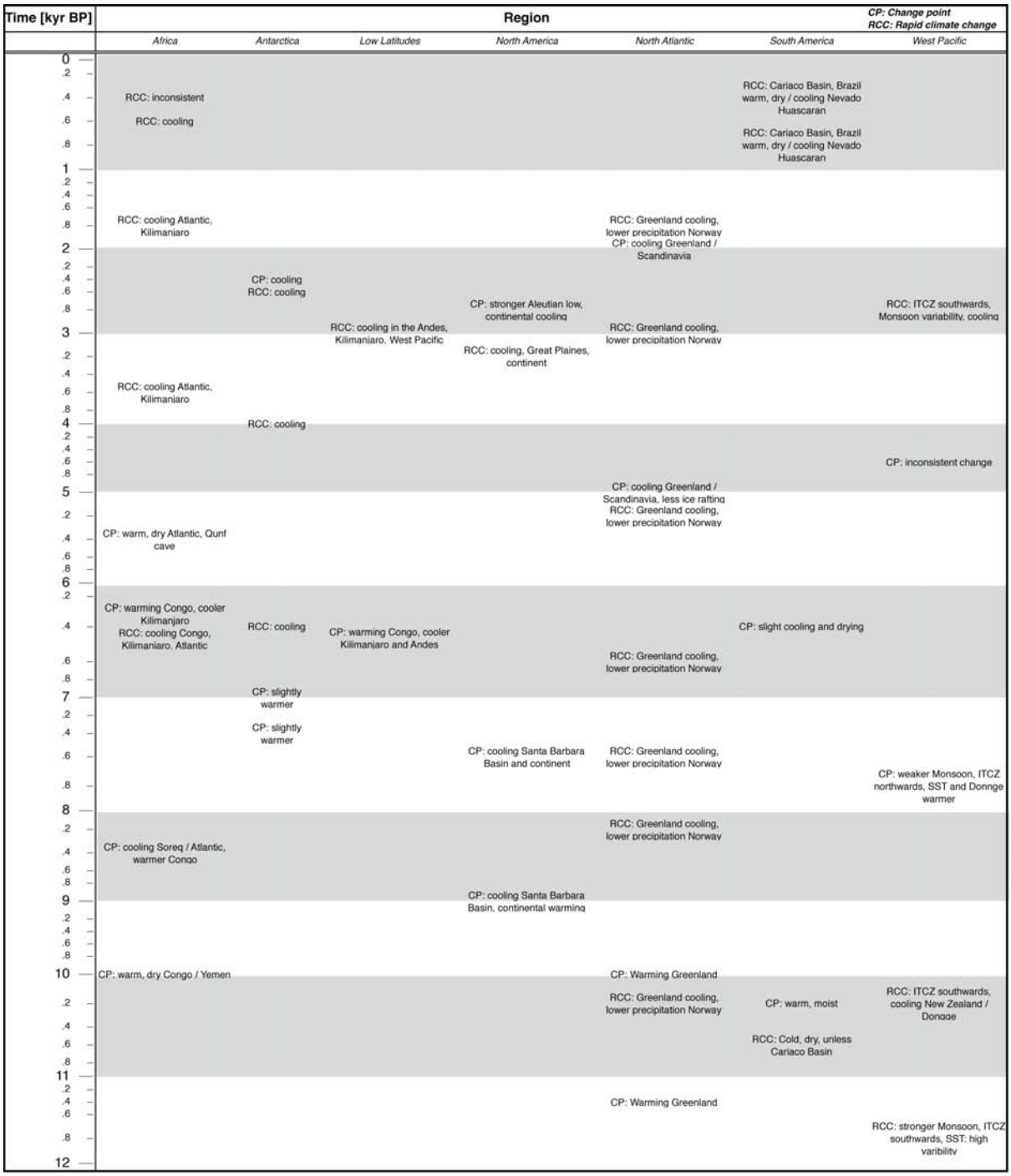

Figure 22: A global synopsis of RCC and change point analysis

5 Discussion

In this chapter, the results of the detection of RCC and change points presented in the section 4 are discussed. It will focus on the two most eye-catching events visible in figure 22 at about 2.8 and 6.4 kyr BP. The chapter is concluded with the results of the North Atlantic region and an attempt to link them with the theory about the postulated 1500-year cycle, it's spatial extent and possible forcing mechanisms.

5.1 Evaluation of the applied methods

The main purpose of this study was to assess significant changes and phases of rapid climate change in mostly temperature- and precipitation-sensitive climate proxies in order to find out more about the occurrence and spatial extent of a postulated 1500-year cycle in climate. The results of RCC detection in the ice rafting proxy by Bond et al. [2001] proofed the suitability of the detection method. It indicated a phase of RCC for each proposed Bond-event, however it always occurred at the end of the ice-rafting event. This would imply, that the warming would be faster than the foregoing cooling.

The change point analysis did not detect all the phases, which were considered as Bond events. The analysis of the IRD time series only showed three phases and two significant change points throughout the Holocene. The sum of all change points of a region however results in a clearer picture of possible climate cycles.

5.2 Comparison of the results with paleoclimatic events

5.2.1 The 2.8 kyr BP - cluster

During the period of 3.2 – 2.8 kyr BP, our results show several summations of RCC and change points in the Northern Hemisphere. The North American region shows a rapid continental cooling 3.2 kyr BP and a beginning phase of lower temperatures 2.8 kyr BP connected with a weaker Aleutian low. The analysis of the North Atlantic region revealed a rapid cooling 3 kyr BP in Greenland and at the same time decreasing precipitation in Norway. In the West Pacific, the ITCZ is moving southwards whereas the East Asian Monsoon is showing high variability. New Zealand and the West Pacific SST show a rapid cooling around 3 kyr BP (figure 23). Rapid cooling in the North Atlantic and a decrease in precipitation in Northern Europe were also mentioned in other studies [e.g. *Andersen et al.,* 2004; *Plunkett and Swindles,* 2008; *Swindles et al.,* 2007] and was related to the low solar activity around 2.8 kyr BP. A recent reconstruction of solar activity confirms this low solar activity [*Steinhilber et al.,* 2009]. The event coincides with one of the peaks in ice rafting in the North Atlantic [*Bond et al.,* 2001].

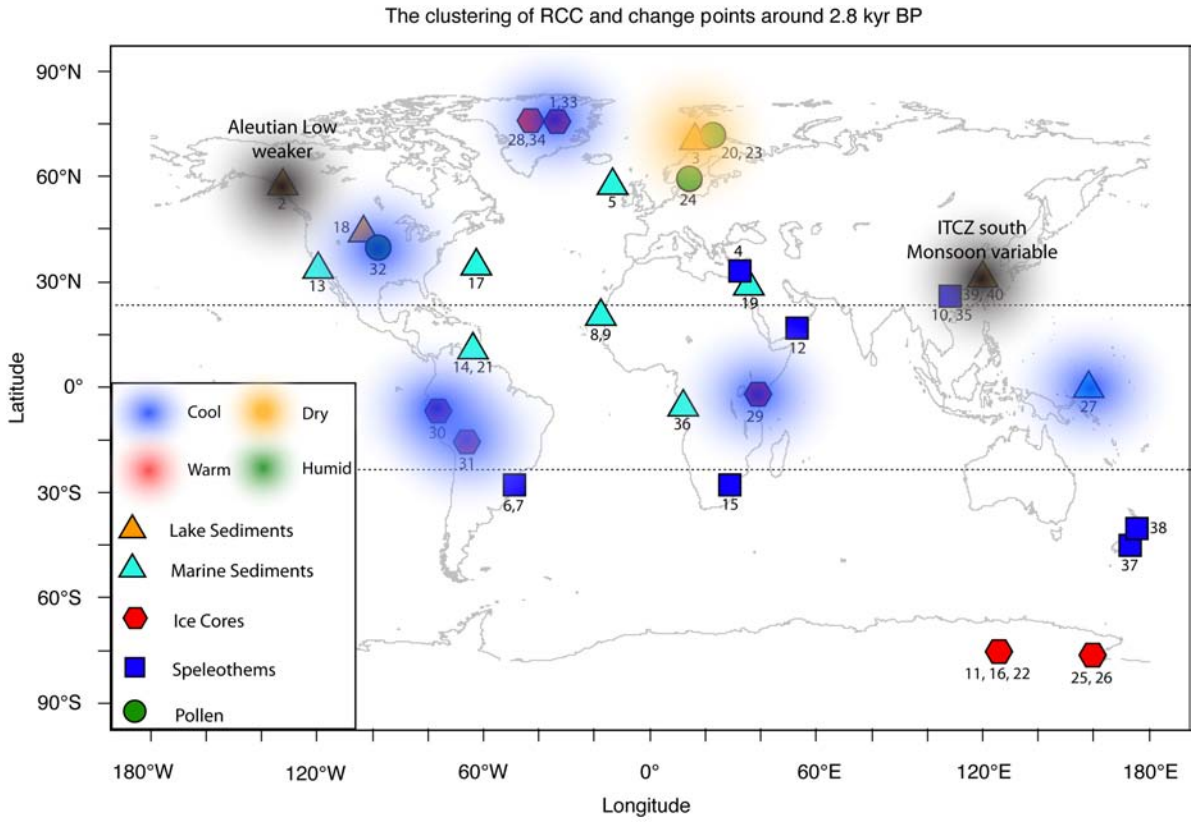

Figure 23: Clustering of RCC and change points around 2.8 kyr BP

Figure 24 shows a conceptual model of large-scale interconnections between surface temperature, monsoon, solar activity and melt water outburst on centennial to millennial timescale by Hong et al. [2009]. They claimed that reduced solar activity and melt water outburst are the two main triggering factors for the repeating pattern of abrupt temperature und humidity anomalies with global extent. For our summary of changes around 2.8 kyr BP, a large-scale melt-water outbreak can be excluded, since no geological evidence is known.

The model by Hong et al. [2009] assumes that downward – penetrating effects triggered by changes in stratospheric ozone would lead to North Hemisphere cooling, above all in the high latitudes [*Bond et al.*, 2001; *Haigh*, 1996; *Shindell et al.*, 1999].

As a consequence, the latitudinal temperature gradient decreases leading to less developed low-pressure systems along the polar frontal zone. Our analysis shows a beginning phase of a weak Aleutian low starting at 2.8 kyr BP.

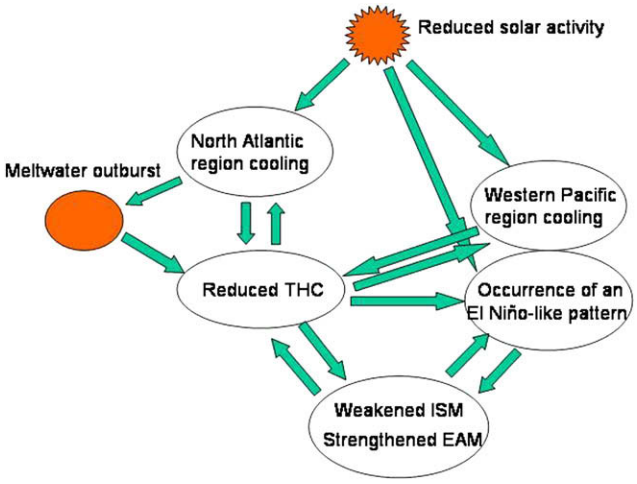

Figure 24: Climatic interconnections on centennial to millennial timescales [*Hong et al.*, 2009]

A weakening of the semi-permanent low-pressure systems is commonly accompanied by negative North Atlantic Oscillation (NAO) indices. The rapid decrease in rainfall in Finland supports this theory. Furthermore, Plunkett and Swindles [2008] and Swindles et al. [2007] revealed the beginning of a dry period in Ireland and also claimed it to be caused by the decreasing solar activity. In the context of lower NAO indices, this is caused by a strong Siberian high-pressure system and weakened and more southerly located westerlies. The advection of moist air masses hence rather affects Central and Southern Europe. Usually, a negative NAO index means higher temperatures for Southern Greenland and the SST off its coast. Our analyses however show a rapid temperature relapse and a significant change point marking a beginning phase of lower temperature in Greenland. We assume that the lower solar irradiance is hence dominating the local NAO-like pattern.

Furthermore, studies and modeling has shown that the SST in the Western Pacific would decrease as well, resulting in El Niño-like conditions. This pattern on the other hand, leads to a weakening of the Indian Summer Monsoon (ISM) and to a strengthening of the East Asian Monsoon (EAM).

Moreover, Wanner et al. [2008] pointed to a southward shift of the ITCZ following a large-scale cooling of the Northern Hemisphere. Our analysis confirms this view; the detection of RCC shows a rapid movement of the ITCZ in the West Pacific region towards the South. Although the proxy for the EAM by Wang et al. [2005] does not show a significant change point or RCC at this time, a weakening in the strength of the EAM is clearly visible in the data (figures 14 and 21).

Our analyses show a decrease in temperature for the two proxies in the Andes, although El Niño-like conditions lead to increased temperatures along the South American west coast. We assume that – analogously to the North Atlantic – the local climate pattern is also dominated by the decrease in solar radiation.

5.2.2 The 6.4 kyr BP - cluster

Figure 25 shows the cluster of change points and RCC around 6.4 kyr BP. The North Atlantic is characterized by a similar scheme as in the aforementioned event around 3 kyr BP: The Greenland ice core proxies show a cooling whereas the rainfall in Finland decreased. Unlike the 3 kyr BP event, the tropics and the southern hemisphere were more affected by changes at this time: Several proxies in tropical Africa and South America indicate colder and drier conditions. Furthermore, Gasse [2000] revealed a rapid change towards dryer conditions in Africa around 6.4 kyr BP, derived from an Ethiopian lake level record.

The Antarctica indicates a summation of rapid cooling events. Additionally, Andersen et al. [2004] report a rapid cooling of the Irminger current off the southwest coast of Iceland at that time. In contrast to the 2.8 kyr BP clustering, the trigger for this occurrence of global extent is still under debate. External forces like the sun's radiative output, internal dynamics in the ocean circulation system and large-scale variations in atmospheric processes as well as volcanic activity are under debate.

Abram et al. [2009] investigated the importance of the Indo-Pacific Warm Pool (IPWP) and it's influence and coupling to global climate. Their reconstruction of the SST in the western tropical Pacific Ocean, the Indonesian archipelago and the eastern tropical Indian Ocean is based on modern and fossil coral records and shows an abrupt, short lived shift to warmer SST between 6.6 and 6.3 kyr BP and also during other periods in Holocene. They pointed to the key role of the IPWP in the propagation of climate changes through its influence on global distribution of heat and water vapor and especially on the Indian Ocean Dipole (IOD), which is a coupled oceanic and atmospheric phenomenon in the equatorial Indian Ocean. Warmer SST in the IPWP hence reflects cooler and dryer conditions in the East Indian Ocean. The proxies by Thompson [2002] and Gasse [2000] support this finding.

Our result in the Nevado Huascaran showing a change-point towards cooler conditions is possibly coupled with mid-Holocene changes in the ENSO pattern. Abram et al. [2009 and references therein] pointed to proxy records from around the Pacific, which consistently suggest a reduction of variability and strength of the El Niño events in the mid-Holocene. For the Andes region this would lead to lower temperatures and dryer conditions.

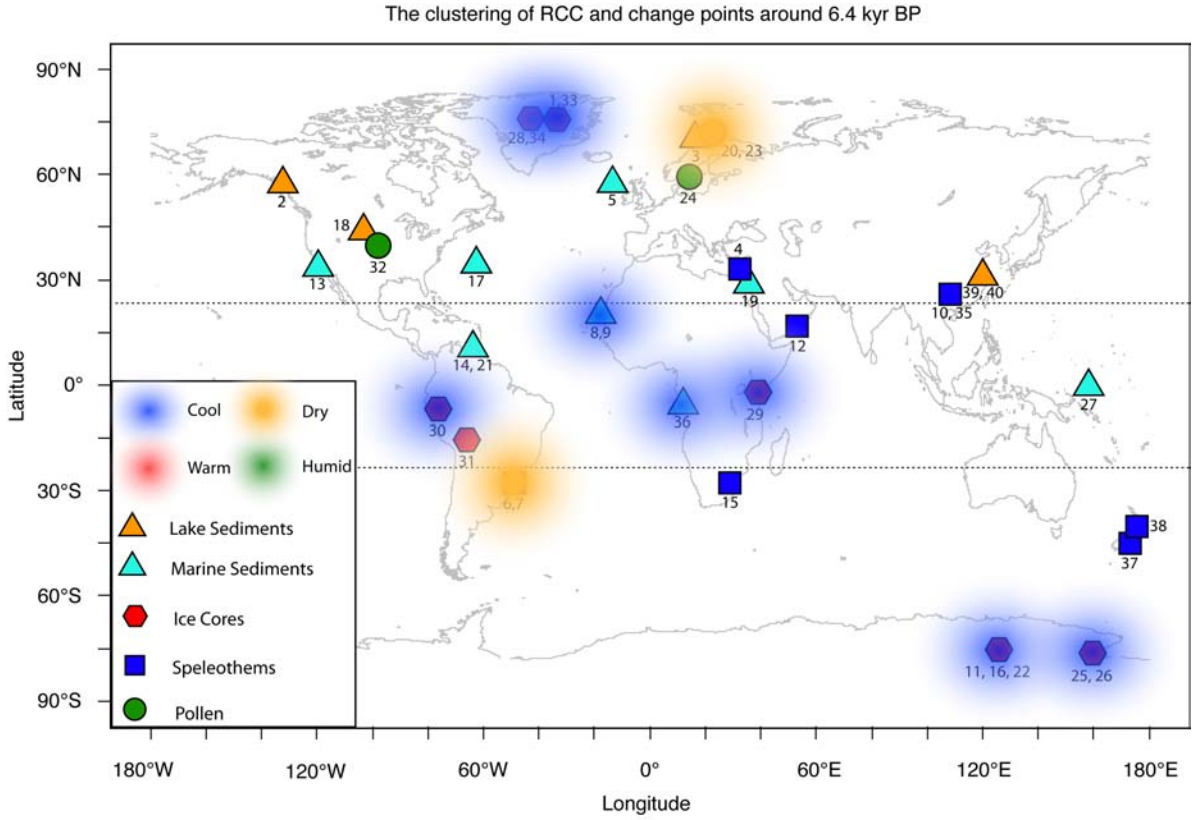

Figure 25: Clustering of RCC and change points around 6.4 kyr BP

5.2.3 The North Atlantic cyclic summation of RCC and change points

The comparison of the proxies related to the Holocene ice rafting [*Bond et al.*, 2001] based on our detection of RCC (figure 26) shows that the first five ice rafting events in the early Holocene went along with summations of rapid climate change in different proxies. The timing of the change points however is not consistent. The analysis on the IRD-time series itself indicates a rapid decrease in ice rafting after each peak, hence rather a rapid warming, whereas most of the detected RCC in the temperature-sensitive proxies point towards a rapid cooling. The reconstruction of precipitation in Norway by Bakke et al. [2005] shows extensive fluctuations during the early Holocene, yet they occur not to coincide with the ice rafting.

The most eye-catching event in the early Holocene is centered around 8.2 kyr BP and most likely related to the glacial lake outburst flood of the Lake Agassiz into the North Atlantic [*Alley and Agustsdottir*, 2005]. Our detection of RCC showed a rapid change towards cooler conditions in three of the four temperature-sensitive proxies. Precipitation in Norway indicates a decrease and the ice rafting a peak around the time of the flood outburst. The change point analysis indicating higher temperature after the event the Greenland ice cores

points to about 250 years of recovery time after the event. Model simulations by Alley and Agustsdottir [2005] show a bipolar seesaw-like increase in SST in the Antarctic Ocean and East Antarctica following the dramatic outburst flood in the North Atlantic. Our analyses however did not trap them.

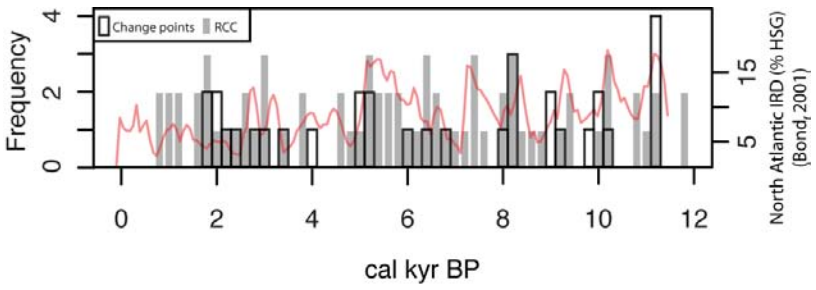

Figure 26: Summary of the change points and RCC in the North Atlantic Region compared with the ice rafting proxy (red curve) by Bond et al. [2001]

In the past 6 kyr, our analyses do not correspond with the IRD proxy any more. A cluster of RCC towards lower temperature centered at 5.2 kyr BP and four change points indicating a beginning phase of cooler temperature in Greenland and Sweden are not concordant with the IRD proxy, which indicates a rapidly decreasing intensity in ice rafting. A further peak around 2 kyr BP indicates a dropping temperature and more arid conditions in Norway. Ice rafting however was constantly at a low level that time. The most recent cluster of RCC appears 1.2 kyr BP and indicates mainly two minor cold relapses in Greenland in one proxy, which does not correspond with the IRD time series. Summarized, our analyses of RCC and change points in the North Atlantic agree well with the ice rafting proxy throughout the early Holocene, a match in the past 6 kyr however is not clearly visible.

Wanner and Bütikofer [2008] introduced a possible mechanism for the formation of the cold event during the late Holocene (see figure 27). They claimed the events to be primarily caused by decreasing incoming solar radiation as a combination of reduced Milankovich forcing (see chapter 1.2.3.1), weakened solar activity and the accumulation of multiple volcanic eruptions. The reduced solar irradiance in the high latitudes of the Northern hemisphere then results in cooler SST and a strengthening of the polar surface anticyclone. The increased amount of sea ice would consequently slowly reduce the deep convection in the North Atlantic and would in turn reduce the SST in the Northern Oceans. A sea ice-albedo feedback [*Curry et al.*, 1995] mechanism on the other hand could explain our indications of a rapid decrease of ice rafting after each peak, although these only occurred in the early Holocene.

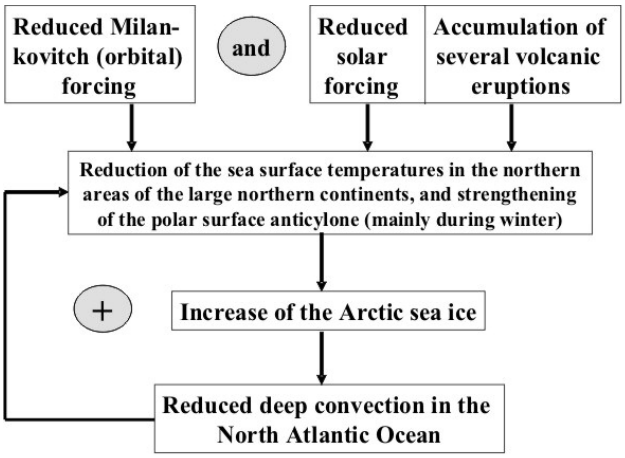

Figure 27: Possible mechanism for the formation of the cold event during the late Holocene [*Wanner and Bütikofer*, 2008]

5.3 Synthesis

The closer look to three specific events and a specific region demonstrates, that Holocene climate showed some considerable regional and global variability on different timescales. The quasiperiodic phases of enhanced ice rafting in the North Atlantic, visible in the IRD proxy by Bond et al. [2001], could also be found in other proxies in this region, however there is no evidence of a cyclic forcing factor nor indications for an internal variability causing this periodicity. The signal of cycles decreases in the late Holocene.

Our analyses pointed to two main events of changes with global extent. The first event around 2.8 kyr BP is most likely caused by a decrease in solar activity, combined with the reduced orbital forcing. The changes in our proxies fit well to a conceptual model by Hong et al. [2009] on the interconnections between surface temperature, monsoon, solar activity, the thermohaline circulation and melt water outburst on centennial to millennial timescales.

Also Abram et al. [2009] pointed to the importance of large-scale climate patterns for the characteristics of centennial to millennial scale climate change. They examined past changes of the Indopacific Warm Pool and its influence to the Indian Ocean Dipole and the ENSO pattern. One of their described peaks is also depicted in our analyses and showed large-scale cooling in the tropics as well as in the Polar Regions 6.4 kyr BP.

However, the analyses have shown that each event has an individual footprint and that regional interactions are diverse for each large-scale event.

The forcing factors of the trapped events are still under debate and most likely not consistent in time. Mayewski et al. [2004] presented a variety of possible causes of Holocene climate

change on local to global scale. They subdivided the Holocene into three segments of different dominating forcing factors and claimed the early Holocene to be dominated by the ice sheet extent and multiple glacier lake outbursts into the North Atlantic. A probably enhanced production of sea ice after the northern hemispheric early Holocene maximum in solar insolation (see figure 2) provided an additional positive feedback to climate cooling.

There is no evidence for large freshwater outbreaks in the past 8 kyr BP and no indication of considerable change in greenhouse gas concentrations until industrial times [*Mayewski et al.*, 2004]. Solar variability is hence the most plausible forcing for this period, especially since the described 3 kyr event coincides with a period of low solar activity [*Steinhilber et al.*, 2009]. The volcanic impact on climate is difficult to estimate, since there is only little data, which enables the reconstruction of volcanic activity throughout the past millennia. Wanner et al. [2008] pointed to the intensifying potential of coincidental low solar activity and volcanic activity to decadal to multi-centennial timescale climate, as it occurred during the Medieval Warm Period.

6 Conclusions and outlook

This study aimed to compare multiple paleoclimatic records of the past 12 kyr using change point analysis and a method to detect rapid climate change. Forty proxies, subdivided in regions of continental extent, were analyzed in order to catch dominant regional to global patterns and possible cyclicities of climate change over the past 12 kyr. Specially focused was the North Atlantic region, where the existence of a consistent cycle throughout the Holocene is under heavy discussion [e.g. *Andrews*, 2006; *Bond et al.*, 1997; *Bond et al.*, 2001; *Bütikofer*, 2007; *Wanner et al.*, 2008; *Wanner and Bütikofer*, 2008].

According to the results presented and discussed in chapter 4 and 5, the questions raised in the objective (see chapter 1.4) can be answered as follows:

Are there signs of regionally coinciding phases of rapid climate change?

The detection of RCC events indicated multiple significant events in several regions. Temporal clustering of change points was observed as well. The composite result of RCC and change points revealed several events of global extent, most likely originating of decrease in solar insolation.

Can signals of a potential millennial-scale cycle in the North Atlantic be trapped?

The summation of RCC events in the North Atlantic region showed an increase during the phases of intensive ice rafting during the first five “Bond events” in the early Holocene from 12 to 7.5 kyr BP. Glacier lake outbursts into the North Atlantic, which caused changes in the thermohaline circulation are assumed to be the main triggering factor for these multiple cold relapses. The signals of a climatic cycle in the late Holocene were weaker in the analyses performed and the query regarding the causes of the changes in North Atlantic climate showed that at least two major cooling events, the LIA and the 2.8 kyr event, were most likely related to solar variability. Due to the lack of data, the influence of volcanic eruptions could not be assessed more closely. Yet it is assumed that the accumulation of several volcanic eruptions in a short period plays a considerable role in fortifying the reduction of TSI due to Milankovich forcing and low solar activity. Indications of a global climate cycle could not be found.

Do the detected phases of rapid climate change and the change points in climatic time-series reveal any spatial patterns of climate change?

The closer analysis of events centered at 2.8 and 6.4 kyr BP pointed toward the importance of long-term changes in climatic patterns, which also influence the regional climate on annual to decadal scale. Changes in North Atlantic's climate on centennial timescale appear like NAO changes on annual timescale, with certain differences however. The tropic changes seem to be heavily influenced by changes in the IPWP, which propagates via the ENSO to the South Pacific and via the IOD to the Indian Ocean and to the African continent.

We are aware that this thesis only catches a small amount of the complexity of Holocene climate on centennial to millennial timescale. However, we are convinced that the performed analyses confirmed and questioned certain previous assumptions.

We consider this thesis as a continuation of the diploma thesis by Bütikofer [2007], who focused on tracking possible Bond cycles using spectral analysis of multiple proxies of the past 6 kyr. He stated that his resulting power spectra seemed to be rather unrelated with each other. After applying our methods we can support these findings since we primarily found relations and teleconnections based on single events with no periodical recurrence. Since we have learned that there are still many uncertainties in Holocene climate variability, further research in detecting the driving mechanisms of the postglacial climate is crucial. The long-term changes of main triggers of climate variability like solar variability and the mechanisms behind high and low volcanic activity are still very little known and there is still much to discover about these forcing factors itself. The future research about the climatic impact of the forcing factors will hopefully get away of simplistic comparisons with the generally cited reference work by Bond et al. [2001] and rather focus on disentangling the complex picture of multiproxy datasets, which are rounded off by new proxies of high temporal resolution. In addition, these analyses would help the numerical climate models to be calibrated more accurately, what would increase our knowledge about the climate in Holocene. A knowledge, which is crucial in a world, where the climate change is probably the biggest challenge of the upcoming centuries.

7 References

Abram, N. J., H. V. McGregor, M. K. Gagan, W. S. Hantoro, and B. W. Suwargadi (2009), Oscillations in the southern extent of the Indo-Pacific Warm Pool during the mid-Holocene, *Quaternary Science Reviews*, *28*(25-26), 2794-2803.

Alley, R. B., P. A. Mayewski, T. Sowers, M. Stuiver, K. C. Taylor, and P. U. Clark (1997), Holocene climatic instability: A prominent, widespread event 8200 yr ago, *Geology*, *25*(6), 483-486.

Alley, R. B. (2000), The Younger Dryas cold interval as viewed from central Greenland, *Quaternary Science Reviews*, *19*(1-5), 213-226.

Alley, R. B., and A. M. Agustsdottir (2005), The 8k event: cause and consequences of a major Holocene abrupt climate change, *Quaternary Science Reviews*, *24*(10-11), 1123-1149.

Ammann, C. M., F. Joos, D. S. Schimel, B. L. Otto-Bliesner, and R. A. Tomas (2007), Solar influence on climate during the past millennium: Results from transient simulations with the NCAR Climate System Model, *Proceedings of the National Academy of Sciences of the United States of America*, *104*(10), 3713-3718.

Andersen, C., N. Koc, and M. Moros (2004), A highly unstable Holocene climate in the subpolar North Atlantic: evidence from diatoms, *Quaternary Science Reviews*, *23*(20-22), 2155-2166.

Anderson, L., M. B. Abbott, B. P. Finney, and S. J. Burns (2005), Regional atmospheric circulation change in the North Pacific during the Holocene inferred from lacustrine carbonate oxygen isotopes, Yukon Territory, Canada, *Quaternary Research*, *64*(1), 21-35.

Andrews, J. J., A.; Moros, M.; Hillaire-Marcel, C.; Eberl, D. (2006), Is there a pervasive Holocene ice-rafted debris (IRD) signal in the Northern Atlantic? The answer appears to be either no, or it depends on the proxy!, *PAGES News*, *14*(2), 7-9.

Bakke, J., S. O. Dahl, O. Paasche, R. Lovlie, and A. Nesje (2005), Glacier fluctuations, equilibrium-line altitudes and palaeoclimate in Lyngen, northern Norway, during the Lateglacial and Holocene, *Holocene*, *15*(4), 518-540.

Bar-Matthews, M., A. Ayalon, M. Gilmour, A. Matthews, and C. J. Hawkesworth (2003), Sea-land oxygen isotopic relationships from planktonic foraminifera and speleothems in the Eastern Mediterranean region and their implication for paleorainfall during interglacial intervals, *Geochimica Et Cosmochimica Acta*, *67*(17), 3181-3199.

Bauer, E. (2005), Klimafaktoren und Klimaänderungen im letzten Jahrtausend, *Sterne und Weltraum*, *44*(12), 31-38.

Beer, J., W. Mende, and R. Stellmacher (2000), The role of the sun in climate forcing, *Quaternary Science Reviews*, *19*(1-5), 403-415.

Beer, J., M. Vonmoos, and R. Muscheler (2006), Solar variability over the past several millennia, *Space Science Reviews*, *125*(1-4), 67-79.

Bond, G., W. Showers, M. Cheseby, R. Lotti, P. Almasi, P. deMenocal, P. Priore, H. Cullen, I. Hajdas, and G. Bonani (1997), A pervasive millennial-scale cycle in North Atlantic Holocene and glacial climates, *Science*, *278*(5341), 1257-1266.

Bond, G., B. Kromer, J. Beer, R. Muscheler, M. N. Evans, W. Showers, S. Hoffmann, R. Lotti-Bond, I. Hajdas, and G. Bonani (2001), Persistent solar influence on north Atlantic climate during the Holocene, *Science*, *294*(5549), 2130-2136.

Bradley, R. S. (1996), *Quaternary paleoclimatology : methods of paleoclimatic reconstruction*, 5th ed., 472 pp., Chapman and Hall, London.

Bütikofer, J. (2007), Millenial scale climate variability during the last 6000 years - tracking down the Bond cycles, Diplomarbeit thesis, 138 pp, University of Bern, Bern.

Craig, H. (1961), Standard for Reporting Concentrations of Deuterium and Oxygen-18 in Natural Waters, *Science*, *133*(346), 1833-1834.

Crowley, T. J. (2000), Causes of climate change over the past 1000 years, *Science*, *289*(5477), 270-277.

Cruz, F. W., S. J. Burns, I. Karmann, W. D. Sharp, M. Vuille, A. O. Cardoso, J. A. Ferrari, P. L. S. Dias, and O. Viana (2005), Insolation-driven changes in atmospheric circulation over the past 116,000 years in subtropical Brazil, *Nature*, *434*(7029), 63-66.

Curry, J. A., J. L. Schramm, and E. E. Ebert (1995), Sea-Ice Albedo Climate Feedback Mechanism, *Journal of Climate*, *8*(2), 240-247.

Dansgaard, W., S. J. Johnsen, H. B. Clausen, D. Dahljensen, N. S. Gundestrup, C. U. Hammer, C. S. Hvidberg, J. P. Steffensen, A. E. Sveinbjornsdottir, J. Jouzel, and G. Bond (1993), Evidence for General Instability of Past Climate from a 250-Kyr Ice-Core Record, *Nature*, *364*(6434), 218-220.

deMenocal, P. B., J. Ortiz, T. Guilderson, and M. Sarnthein (2000), Coherent high- and low-latitude climate variability during the holocene warm period, *Science*, *288*(5474), 2198-2202.

deMenocal, P. B. (2001), Cultural responses to climate change during the Late Holocene, *Science*, *292*(5517), 667-673.

Denton, G. H., and W. Karlen (1973), Holocene climatic variations? Their pattern and possible cause, *Quaternary Research*, *3*(2), 155-174.

Dykoski, C. A., R. L. Edwards, H. Cheng, D. X. Yuan, Y. J. Cai, M. L. Zhang, Y. S. Lin, J. M. Qing, Z. S. An, and J. Revenaugh (2005), A high-resolution, absolute-dated Holocene and deglacial Asian monsoon record from Dongge Cave, China, *Earth and Planetary Science Letters*, *233*(1-2), 71-86.

EPICA Community Members (2007), Methane and stable isotope record of ice core EDML from Dronning Maud Land, Antarctica, http://doi.pangaea.de/10.1594/PANGAEA.586834 (Accessed: 2009.11.29).

Esper, J., E. R. Cook, and F. H. Schweingruber (2002), Low-frequency signals in long tree-ring chronologies for reconstructing past temperature variability, *Science*, *295*(5563), 2250-2253.

Fleitmann, D., S. J. Burns, M. Mudelsee, U. Neff, J. Kramers, A. Mangini, and A. Matter (2003), Holocene forcing of the Indian monsoon recorded in a stalagmite from Southern Oman, *Science*, *300*(5626), 1737-1739.

Fleitmann, D., S. J. Burns, A. Mangini, M. Mudelsee, J. Kramers, I. Villa, U. Neff, A. A. Al-Subbary, A. Buettner, D. Hippler, and A. Matter (2007), Holocene ITCZ and Indian monsoon dynamics recorded in stalagmites from Oman and Yemen (Socotra), *Quaternary Science Reviews*, *26*(1-2), 170-188.

Friddell, J. E., R. C. Thunell, T. P. Guilderson, and M. Kashgarian (2003), Increased northeast Pacific climatic variability during the warm middle Holocene, *Geophysical Research Letters*, *30*(11), 1560-1563.

Gascoyne, M. (1992), Paleoclimate determination from cave calcite deposits., *Quaternary Science Reviews*, *11*, 609-632.

Gasse, F. (2000), Hydrological changes in the African tropics since the Last Glacial Maximum, *Quaternary Science Reviews*, *19*(1-5), 189-211.

Grootes, P. M., M. Stuiver, J. W. C. White, S. Johnsen, and J. Jouzel (1993), Comparison of Oxygen-Isotope Records from the Gisp2 and Grip Greenland Ice Cores, *Nature*, *366*(6455), 552-554.

Haigh, J. D. (1996), The impact of solar variability on climate, *Science*, *272*(5264), 981-984.

Hansen, J., M. Sato, R. Ruedy, A. Lacis, K. Asamoah, S. Borenstein, E. Brown, B. Cairns, G. Caliri, and M. Campbell (1996), A Pinatubo climate modeling investigation, *In: The Mount Pinatubo eruption: Effects on the atmosphere and climate*, *Nato a S I Series, Global and Environmental Change*, 232-272.

Haug, G. H., K. A. Hughen, D. M. Sigman, L. C. Peterson, and U. Rohl (2001), Southward migration of the intertropical convergence zone through the Holocene, *Science*, *293*(5533), 1304-1308.

Hays, J. D., J. Imbrie, and N. J. Shackleton (1976), Variations in Earths Orbit - Pacemaker of Ice Ages, *Science*, *194*(4270), 1121-1132.

Hegerl, G. C., T. J. Crowley, S. K. Baum, K. Y. Kim, and W. T. Hyde (2003), Detection of volcanic, solar and greenhouse gas signals in paleo-reconstructions of Northern Hemispheric temperature, *Geophysical Research Letters*, *30*(5).

Hinkley, D. V. (1971), Inference About Change-Point from Cumulative Sum Tests, *Biometrika*, *58*(3), 509-523.

Holmgren, K., J. A. Lee-Thorp, G. R. J. Cooper, K. Lundblad, T. C. Partridge, L. Scott, R. Sithaldeen, A. S. Talma, and P. D. Tyson (2003), Persistent millennial-scale climatic variability over the past 25,000 years in Southern Africa, *Quaternary Science Reviews*, *22*(21-22), 2311-2326.

Hong, Y. T., B. Hong, Q. H. Lin, Y. Shibata, Y. X. Zhu, X. T. Leng, and Y. Wang (2009), Synchronous climate anomalies in the western North Pacific and North Atlantic regions during the last 14,000 years, *Quaternary Science Reviews*, *28*(9-10), 840-849.

IPCC (2007), *Climate Change 2007: The Physical Science Basis*, Intergovernmental Panel on Climate Change, Geneva.

Jones, P. D., and M. E. Mann (2004), Climate over past millennia, *Reviews of Geophysics*, *42*(2).

Jouzel, J., L. Merlivat, J. R. Petit, and C. Lorius (1983), Climatic information over the last century deduced from a detailed isotopic record in the South Pole snow, *Journal of Geophysical Research*, *88(C4)*, 2693-2703.

Jouzel, J., V. Masson, O. Cattani, S. Falourd, M. Stievenard, B. Stenni, A. Longinelli, S. J. Johnsen, J. P. Steffenssen, J. R. Petit, J. Schwander, R. Souchez, and N. I. Barkov (2001), A new 27 ky high resolution East Antarctic climate record, *Geophysical Research Letters*, *28*(16), 3199-3202.

Keigwin, L. D. (1996), The Little Ice Age and Medieval warm period in the Sargasso Sea, *Science*, *274*(5292), 1504-1508.

Laird, K. R., S. C. Fritz, E. C. Grimm, and P. G. Mueller (1996), Century-scale paleoclimatic reconstruction from Moon Lake, a closed-basin lake in the northern Great Plains, *Limnology and Oceanography*, *41*(5), 890-902.

Lamy, F., H. W. Arz, G. C. Bond, A. Bahr, and J. Patzold (2006), Multicentennial-scale hydrological changes in the Black Sea and northern Red Sea during the Holocene and the Arctic/North Atlantic oscillation, *Paleoceanography*, *21*(1).

Larocque, I., and R. I. Hall (2004), Holocene temperature estimates and chironomid community composition in the Abisko,Valley, northern Sweden, *Quaternary Science Reviews*, *23*(23-24), 2453-2465.

Laskar, J., P. Robutel, F. Joutel, M. Gastineau, A. C. M. Correia, and B. Levrard (2004), A long-term numerical solution for the insolation quantities of the Earth, *Astronomy & Astrophysics*, *428*(1), 261-285.

Lea, D. W., D. K. Pak, L. C. Peterson, and K. A. Hughen (2003), Synchroneity of tropical and high-latitude Atlantic temperatures over the last glacial termination, *Science*, *301*(5638), 1361-1364.

Mann, M. E., R. S. Bradley, and M. K. Hughes (1999), Northern hemisphere temperatures during the past millennium: Inferences, uncertainties, and limitations, *Geophysical Research Letters*, *26*(6), 759-762.

Matthes, F. E. (1939), Report of committee on glaciers, *Transactions-American Geophysical Union*, *20*, 518-523.

Mayewski, P. A., E. E. Rohling, J. C. Stager, W. Karlen, K. A. Maasch, L. D. Meeker, E. A. Meyerson, F. Gasse, S. van Kreveld, K. Holmgren, J. Lee-Thorp, G. Rosqvist, F. Rack, M. Staubwasser, R. R. Schneider, and E. J. Steig (2004), Holocene climate variability, *Quaternary Research*, *62*(3), 243-255.

Milanković, M. (1930), *Mathematische Klimalehre und astronomische Theorie der Klimaschwankungen*, Borntraeger, Berlin.

Moberg, A., D. M. Sonechkin, K. Holmgren, N. M. Datsenko, and W. Karlen (2005), Highly variable Northern Hemisphere temperatures reconstructed from low- and high-resolution proxy data, *Nature*, *433*(7026), 613-617.

Muscheler, R., F. Joos, J. Beer, S. A. Muller, M. Vonmoos, and I. Snowball (2007), Solar activity during the last 1000 yr inferred from radionuclide records, *Quaternary Science Reviews*, *26*(1-2), 82-97.

Nesje, A., and S. O. Dahl (1993), Lateglacial and Holocene Glacier Fluctuations and Climate Variations in Western Norway - a Review, *Quaternary Science Reviews*, *12*(4), 255-261.

Obrien, S. R., P. A. Mayewski, L. D. Meeker, D. A. Meese, M. S. Twickler, and S. I. Whitlow (1995), Complexity of Holocene Climate as Reconstructed from a Greenland Ice Core, *Science*, *270*(5244), 1962-1964.

Osborn, T., and K. R. Briffa (2006), The spatial extent of 20th-century warmth in the context of the past 1200 years, *Science*, *311*(5762), 841-844.

Page, E. S. (1954), Continuos Inspection Schemes, *Biometrika*, *42*(1/2), 16.

Petit, J. R., J. Jouzel, D. Raynaud, N. I. Barkov, J. M. Barnola, I. Basile, M. Bender, J. Chappellaz, M. Davis, G. Delaygue, M. Delmotte, V. M. Kotlyakov, M. Legrand, V. Y. Lipenkov, C. Lorius, L. Pepin, C. Ritz, E. Saltzman, and M. Stievenard (1999), Climate and atmospheric history of the past 420,000 years from the Vostok ice core, Antarctica, *Nature*, *399*(6735), 429-436.

Pfister, C., J. Luterbacher, D. Brändli, H. Wanner, B. Brodbeck, and P.-A. Nielson (1999), *Wetternachhersage : 500 Jahre Klimavariationen und Naturkatastrophen (1496-1995)*, 304 pp., Verlag Paul Haupt, Bern.

Piciotto, E., X. De Maere, and I. Friedman (1960), Isotopic composition and temperature of formation of Antarctic snows, *Nature*, *187*, 857-859.

Plunkett, G., and G. T. Swindles (2008), Determining the Sun's influence on Lateglacial and Holocene climates: a focus on climate response to centennial-scale solar forcing at 2800 cal. BP, *Quaternary Science Reviews*, *27*(1-2), 175-184.

Robock, A. (2002), Volcanic eruptions and climate, *Climate Change: Natural forcing factors for climate change timescales 10- 1 to 10- 5 years*, *38*, 305.

Roedel, W. (1994), *Physik unserer Umwelt: Die Atmosphäre*, 2nd, revised and updated ed., 467 pp., Springer-Verlag, Berlin.

Seppa, H., and H. J. B. Birks (2002), Holocene climate reconstructions from the fennoscandian tree-line area based on pollen data from Toskaijavri, *Quaternary Research*, *57*(2), 191-199.

Seppa, H., D. Hammarlund, and K. Antonsson (2005), Low-frequency and high-frequency changes in temperature and effective humidity during the Holocene in south-central Sweden: implications for atmospheric and oceanic forcings of climate, *Climate Dynamics*, *25*(2-3), 285-297.

Shindell, D., D. Rind, N. Balachandran, J. Lean, and P. Lonergan (1999), Solar cycle variability, ozone, and climate, *Science*, *284*(5412), 305-308.

Steig, E. J., E. J. Brook, J. W. C. White, C. M. Sucher, M. L. Bender, S. J. Lehman, D. L. Morse, E. D. Waddington, and G. D. Clow (1998), Synchronous climate changes in Antarctica and the North Atlantic, *Science*, *282*(5386), 92-95.

Steinhilber, F., J. Beer, and C. Fröhlich (2009), Total solar irradiance during the Holocene, *Geophysical Research Letters*, *36*(19).

Stott, L., K. Cannariato, R. Thunell, G. H. Haug, A. Koutavas, and S. Lund (2004), Decline of surface temperature and salinity in the western tropical Pacific Ocean in the Holocene epoch, *Nature*, *431*(7004), 56-59.

Stott, P. A., S. F. B. Tett, G. S. Jones, M. R. Allen, J. F. B. Mitchell, and G. J. Jenkins (2000), External control of 20th century temperature by natural and anthropogenic forcings, *Science*, *290*(5499), 2133-2137.

Stuiver, M., P. M. Grootes, and T. F. Braziunas (1995), The GISP2 18O climate record of the past 16,500 years and the role of the sun, ocean and volcanoes. , *Quaternary Research*, *44*, 14.

Swindles, G. T., G. Plunkett, and H. M. Roe (2007), A delayed climatic response to solar forcing at 2800 cal. BP: multiproxy evidence from three Irish peatlands, *Holocene*, *17*(2), 177-182.

Taylor, W. A. (2000), Change-Point Analysis: A Powerful New Tool For Detecting Changes, http://variation.com/cpa/tech/changepoint.html (Accessed: 2009.11.23).

Tett, S. F. B., P. A. Stott, M. R. Allen, W. J. Ingram, and J. F. B. Mitchell (1999), Causes of twentieth-century temperature change near the Earth's surface, *Nature*, *399*(6736), 569-572.

Thompson, L. G., E. Mosleythompson, M. E. Davis, P. N. Lin, K. A. Henderson, J. Coledai, J. F. Bolzan, and K. B. Liu (1995), Late-Glacial Stage and Holocene Tropical Ice Core Records from Huascaran, Peru, *Science*, *269*(5220), 46-50.

Thompson, L. G., M. E. Davis, E. Mosley-Thompson, T. A. Sowers, K. A. Henderson, V. S. Zagorodnov, P. N. Lin, V. N. Mikhalenko, R. K. Campen, J. F. Bolzan, J. Cole-Dai, and B. Francou (1998), A 25,000-year tropical climate history from Bolivian ice cores, *Science*, *282*(5395), 1858-1864.

Thompson, L. G., E. Mosley-Thompson, M. E. Davis, K. A. Henderson, H. H. Brecher, V. S. Zagorodnov, T. A. Mashiotta, P. N. Lin, V. N. Mikhalenko, D. R. Hardy, and J. Beer (2002), Kilimanjaro ice core records: Evidence of Holocene climate change in tropical Africa, *Science*, *298*(5593), 589-593.

Versteegh, G. J. M. (2005), Solar forcing of climate. 2: Evidence from the past, *Space Science Reviews*, *120*(3-4), 243-286.

Viau, A. E., K. Gajewski, M. C. Sawada, and P. Fines (2006), Millennial-scale temperature variations in North America during the Holocene, *Journal of Geophysical Research*, *111*(D9).

Vinther, B. M., H. B. Clausen, S. J. Johnsen, S. O. Rasmussen, K. K. Andersen, S. L. Buchardt, D. Dahl-Jensen, I. K. Seierstad, M. L. Siggaard-Andersen, J. P. Steffensen, A. Svensson, J. Olsen, and J. Heinemeier (2006), A synchronized dating of three Greenland ice cores throughout the Holocene, *Journal of Geophysical Research*, *111*(D13).

Wang, Y. J., H. Cheng, R. L. Edwards, Y. Q. He, X. G. Kong, Z. S. An, J. Y. Wu, M. J. Kelly, C. A. Dykoski, and X. D. Li (2005), The Holocene Asian monsoon: Links to solar changes and North Atlantic climate, *Science*, *308*(5723), 854-857.

Wanner, H., J. Beer, J. Butikofer, T. J. Crowley, U. Cubasch, J. Fluckiger, H. Goosse, M. Grosjean, F. Joos, J. O. Kaplan, M. Kuttel, S. A. Muller, I. C. Prentice, O. Solomina, T. F. Stocker, P. Tarasov, M. Wagner, and M. Widmann (2008), Mid- to Late Holocene climate change: an overview, *Quaternary Science Reviews*, *27*(19-20), 1791-1828.

Wanner, H., and J. Bütikofer (2008), Holocene Bond Cycles - Real or Imaginary?, *Geografie - Sbornik Ceske Geograficke Spolecnosti*, *113*(4), 338-350.

Weijers, J., E. Schefuss, S. Schouten, and J. Damste (2007), Coupled thermal and hydrological evolution of tropical Africa over the last deglaciation, *Science*, *315*(5819), 1701-1704.

Williams, P. W., D. N. T. King, J. X. Zhao, and K. D. Collerson (2004), Speleothem master chronologies: combined Holocene O-18 and C-13 records from the North Island of New Zealand and their palaeoenvironmental interpretation, *Holocene*, *14*(2), 194-208.

Williams, P. W., D. N. T. King, J. X. Zhao, and K. D. Collerson (2005), Late pleistocene to holocene composite speleothem O-18 and C-13 chronologies from south island, new Zealand-did a global younger dryas really exist?, *Earth and Planetary Science Letters*, *230*(3-4), 301-317.

Yancheva, G., N. R. Nowaczyk, J. Mingram, P. Dulski, G. Schettler, J. F. W. Negendank, J. Q. Liu, D. M. Sigman, L. C. Peterson, and G. H. Haug (2007), Influence of the intertropical convergence zone on the East Asian monsoon, *Nature*, *445*(7123), 74-77.

Zielinski, G. A. (2000), Use of paleo-records in determining variability within the volcanism-climate system, *Quaternary Science Reviews*, *19*(1-5), 417-438.

Declaration

under Art. 28 Para. 2 RSL 05

Last, first name:	Grob, Christian
Matriculation number:	04-061-107
Programme:	Master in Climate Sciences
Thesis title:	Holocene climate variability: A proxy-based statistical overview
Thesis supervisors:	Prof. Dr. Heinz Wanner *Institute of Geography, University of Bern and Oeschger Centre for Climate Change Research* Dr. Simon Scherrer *Federal Office of Meteorology and Climatology MeteoSwiss*

I hereby declare that this submission is my own work and that, to the best of my knowledge and belief, it contains no material previously published or written by another person, except where due acknowledgement has been made in the text. In accordance with academic rules and ethical conduct, I have fully cited and referenced all material and results that are not original to this work. I am well aware of the fact that, on the basis of Article 36 Paragraph 1 Letter of the University Law of 5 September 1996, the Senate is entitled to deny the title awarded on the basis of this work if proven otherwise.

Bern, 01.12.2009

Christian Grob